Structure-Activity Relationships of a Novel Group of Large-Conductance Ca²⁺-Activated K⁺ (BK) Channel Modulators: The GoSlo-SR Family

Subhrangsu Roy,[b] Adebola Morayo Akande,[a] Roddy J. Large,[b] Tim I. Webb,[b] Costin Camarasu,[b] Gerard P. Sergeant,[a, b] Noel G. McHale,[a, b] Keith D. Thornbury,[a, b] and Mark A. Hollywood*[a, b]

*a*The Smooth Muscle Research Centre & *b*Ion Channel Biotechnology Centre, Dundalk Institute of Technology, Dublin Road, Dundalk, Co. Louth, Ireland

*Name and address for correspondence:

Mark Hollywood

Smooth Muscle Research Centre
Dundalk Institute of Technology
Dublin Road
Dundalk
Ireland

Tel: (00353) 429370475
Fax: (00353) 429370509
Email: mark.hollywood@dkit.ie
Web: www.smoothmusclegroup.org

Main Text

Large-conductance Ca^{2+}-activated K^+ (BK) channels contribute to the repolarisation or hyperpolarisation of a wide variety of tissues including bladder and urethral smooth muscles.[1-3] In bladder smooth muscle, BK channels are activated by both the influx of Ca^{2+} across the membrane and the release of Ca^{2+} from intracellular stores and are responsible for the rapid repolarisation phase of the action potential. Thus, BK channels help limit the excitability of bladder smooth muscle and consequently reduce its contractile behaviour. Meredith *et al*.,[4] elegantly illustrated the importance of BK channels in controlling bladder contractility by demonstrating that mutant mice, which lack the BKα subunits, have overactive bladders and are functionally incontinent.

It is clear from the above studies that BK channels offer a promising target for the treatment of urinary incontinence caused by overactive bladder (OAB). In this study, we have synthesised a new family of BK channel openers, termed the GoSlo-SR family, that may form scaffold molecules for future development in the treatment of this disease. The predominant cause of OAB is the uncontrolled, inappropriate contraction of the bladder smooth muscle, which increases intravesicle pressure above urethral closure pressure causing urine leakage.[5] The current 'gold standard' therapeutic treatment (anticholinergics) for overactive bladder has compliance rates of <30%, due to unwanted side effects including chronic constipation and dry mouth.[6] Consequently, the pharmaceutical industry has invested significantly in trying to target smooth muscle function by developing novel BK channel modulators to help treat disorders such as urinary incontinence.[6-10]

Although a large number of chemically diverse BK channel openers have already been developed,[8, 9] only a few studies[11-13] have focused on examining the effects of these compounds across a wide voltage range to include physiological potentials ($\sim$–100 mV to 0 mV).[10-12] Instead, the majority of studies have focused on the ability of compounds to open channels only at potentials some 50 to 100 mV more positive than a cell is ever likely to encounter in vivo. It appears that the majority of BK channel openers developed to date would have little effect at physiological membrane potentials and this may explain their poor efficacy in clinical trials[7] and subsequent failure to progress to market.

In this study, we have examined the effects of the GoSlo-SR family of molecules across a wide range of potentials (from −100 mV to +150 mV). In addition, we have chosen to measure efficacy of these BK channel openers by calculating the shift in the voltage required to half maximally activate the channels ($\Delta V_{1/2}$). We have previously used this approach to demonstrate that 10 μM Cibacron Blue (Reactive Blue 2, RB2, see Figure 1A) activated BK channels recorded from bladder smooth muscle cells with $\Delta V_{1/2}$ of $\sim$−50 mV.[11] However, little is known about the minimal structure necessary to retain biological activity on BK channels. In an attempt to address this, we embarked on a molecular reduction strategy to examine which minimal components of RB2 were essential to retain BK channel opening activity. The aims of the present study were therefore to (i) identify the pharmacophore of RB2 for BK channel activation and (ii) investigate the preliminary structure activity relationships of truncated RB2 analogues.

Experimental Section

Single Channel Recording:

In this study, we used the inside-out configuration of the patch clamp technique (see methods in Supporting Information) with symmetrical 140 mM K$^+$ solutions, to evaluate the ability of a series of anthraquinone analogues (**5a-v**, **6**) to open BK channels when applied to the cytosolic surface of membrane patches. When voltage ramps (from –150 mV to +100 mV, –100 mV to +100 mV or –50 mV to +150 mV) were applied to inside-out patches obtained from freshly dispersed rabbit bladder smooth muscle cells and bathed with 100 nM Ca^{2+} at the cytosolic face, a number of distinct, large-conductance (335 ± 5 pS, *n*=9) channel openings could be readily observed at potentials positive to +50 mV. When currents were recorded in the presence of various Ca^{2+} concentrations, the voltage dependence of activation shifted negatively as the [Ca^{2+}] increased. Figures 2A-C show typical single channel currents recorded using the voltage ramps and holding potentials shown in the upper panel of each figure. Note that the currents reversed at 0 mV (the reversal potential for K$^+$ with our recording conditions). When activation curves for the above experiments were constructed and fitted with a Boltzmann equation, the voltage at which the channels were half maximally activated (V$_{1/2}$) was 125 ± 4 mV in 100 nM Ca^{2+} from 22 patches. As Figure 2D suggests, this was shifted negatively to 13 ± 5 mV when the [Ca^{2+}] at the cytosolic face of the channel was increased to 1 μM (p<0.05, *n*=22). Similarly, increasing the [Ca^{2+}] further to 10 μM, shifted the V$_{1/2}$ to –88 ± 6 mV (*n*=12). In a separate series of experiments, we examined the effects of the selective BK channel blocker penitrem A (100 nM, *n*=6)[14] on these large conductance channels. As Figure 2Ei suggests, large conductance channels could be recorded in the presence of 1μM Ca^{2+} at the cytosolic face of the channel and these currents were abolished in the presence of penitrem A (Figure 2Eii) or when iberiotoxin was applied to the extracellular surface of the patch (100 nM, *n*=3, data not shown). Taken together, these data suggest that the large conductance channels recorded in these patches are BK channels and little current remains when BK channels were blocked.

Voltage ramps were also employed in experiments to examine the effects of the novel BK channel openers on these channels. In all of these experiments, the internal surface of the patch was continually bathed with 100 nM Ca^{2+} in the absence and presence of each test

compound and patches were held at -60 mV. In our first set of experiments, we were surprised to observe that the commercially available 1-amino-4-phenylamino-2-sulfoanthraquinone, (Acid Blue 25, AB25, 10 μM, see Figure 1B for structure), was as effective as RB2 and shifted the activation $V_{1/2}$ by -51 ± 10 mV (n=4) compared to -49 ± 11 mV (n=8) in the presence of 10 μM RB2. The phenylamino ring was found to be essential for BK channel activation since 10 μM bromaminic acid (**3**, Scheme 1) failed to activate the channels and actually appeared to have a modest inhibitory effect as evidenced by the positive shift in $\Delta V_{1/2}$ of 14 ± 9 mV (n=5).

Structure Activity Relationship (SAR):

We next designed and synthesised a small library of compounds following a microwave-assisted Ullmann coupling reaction as reported in the literature.[15] We have called these 23 analogues of the lead structure AB25, the GoSlo-SR family. The effect of different substituents on the phenyl ring in the N^4-position was investigated (see Table 1). Eight of the analogues (marked with an asterisk in Table 1) have been reported previously to act as purinoceptor antagonists,[16-18] *ecto*-5′-nucleotidease (*e*N) inhibitors,[19] or ectonucleoside triphosphate diphosphohydrolase (E-NTPDase) inhibitors,[20] but the remainder of the analogues were novel. When we examined the effects of these molecules on BK channels, we found that a significant number of the compounds were efficacious BK channel activators and shifted the activation $V_{1/2}$ in excess of -80 mV (see Table 1). The introduction of an electron donating methyl substituent in the *meta*-position (**5a**)[15, 16, 20] or methoxy group in the *ortho*-position (**5b**)[15, 16, 20] of the phenylamino ring failed to significantly enhance their efficacy on BK channels compared to AB25. However when an ethyl group was substituted in the *ortho*-,[16] *meta*-, or *para*-position (**5c**-**5e**) the ability to shift the voltage required for half maximal activation of the channels was increased approximately two-fold compared to AB25.

Interestingly, the introduction of a bulky hydrophobic isopropyl group in the *ortho*-, *meta*-, and *para*-position (**5f**-**5h**) also increased the efficacy substantially compared to AB25 ($p<0.05$). Among the three regioisomers **5f**-**5h** of the isopropyl substituent, the *ortho* and the *meta*-isomers were more efficacious than the *para*-substituted isomer. Furthermore, we observed that introducing a larger non-polar benzyl substituent in the *meta*-position (**5i**)[18]

had a strong impact on the activity and shifted the $V_{1/2}$ by -120 ± 15 mV ($n=6$) compared to its *para*-isomer[17] (**5j**, $\Delta V_{1/2}$ -79 ± 5 mV, $n=6$).

Introduction of a lipophilic substituent in the *meta*-position of the phenyl ring, such as trifluoromethyl (**5k**), also increased the activity significantly compared to AB25 and shifted the $V_{1/2}$ by -107 ± 7 mV ($n=12$). Figure 3A shows the structure of this compound (which we have called GoSlo-SR-5-6) and Figure 3B shows the typical effect of it when applied to the cytosolic face of the patch at a concentration of 10 µM (Figure 3B, blue trace) in the presence of 100 nM Ca^{2+}. The black trace shows the plot of n.Po (number of channels in patch multiplied by the open probability) obtained in the presence of 1 µM Ca^{2+} to illustrate the maximal number of channel openings in this patch. When these data were fitted with a Boltzmann equation (solid lines) and the activation $V_{1/2}$ was summarised for 12 similar experiments as shown in Figure 3C, **5k** shifted the mean activation $V_{1/2}$ from 122 ± 4 mV in the absence of the drug (gray bar) to 16 ± 7 mV in its presence (blue bar). A change in $[Ca^{2+}]$ to 1 µM (black bar) shifted the $V_{1/2}$ to 23 ± 8 mV in the same patches.

In four separate experiments, we examined if these effects were abolished when BK channels were blocked with penitrem A (100 nM). To quantify this, we elicited currents using the same voltage ramps as above and measured the peak current evoked at +100 mV. In the presence of 100 nM Ca^{2+}, the mean peak current at +100 mV was 160 ± 53 pA and this was significantly increased to 515 ± 95 pA in the presence of **5k**. When penitrem A was added in the continued presence of **5k**, the peak current at +100 mV was reduced to only 12 ± 2 pA ($p<0.05$), consistent with the idea that this molecule mediated its effects via activation of BK channels.

The trifluoromethoxy substituent (**5l**) also had similar effects and shifted the $\Delta V_{1/2}$ by -90 ± 8 mV ($n=6$). Interestingly, substitution of the sulfonate group of **5k** in the C-ring with its isostere carboxyl group (**6**) did not significantly alter its ability to activate the BK channel activity, since this compound still shifted $\Delta V_{1/2}$ by -99 ± 11 mV ($n=7$). However, the commercially available compound, S175099 (Sigma) in which the sulfonate group of AB25 was replaced by a hydrogen atom, was inactive and thus failed to shift the activation $V_{1/2}$ of the BK channels significantly.

The introduction of an electron withdrawing fluorine atom in both the *meta*-positions (**5n**) and the *ortho*-positions (**5o**) of D-ring reduced the ability of these molecules to activate BK channels. The activity was not altered when the D-ring was substituted with electron withdrawing fluorine atom in the single *meta*-position (**5m**). Furthermore, the introduction of a hydrophilic substituent in the *meta*-position such as CO_2H (**5t**)[15, 19] decreased the activity significantly compared to AB25. The combination of a *ortho*-carboxylic acid group with *para*-fluoro substitution (**5v**),[19] known as potent and selective inhibitor of *e*N was found to be inactive towards BK channel. When a nitro group was introduced in the *meta*-position (**5u**),[16, 18] the BK channels activated at more positive voltages, suggesting that it had an inhibitory effect on the channels.

The combination of a *meta*-trifluoromethyl group with *para*-fluoro substitution (**5p**) slightly reduced the efficacy compared to **5k**. The activity of **5q** increased significantly when the chlorine atom replaced the fluorine atom in **5p**. However, a combination of a *meta*-trifluoromethyl group with *para*-methyl substituent furnished the most efficacious compound **5r** in this series, which shifted the activation $V_{1/2}$ by -142 ± 8 mV (*n*=12) when applied at a concentration of 10 μM. Figure 3E shows a typical example of the effect of this compound (which we have called GoSlo-SR-5-44) and allows the direct comparison of its effects with the less efficacious GoSlo-SR-5-6 (Figures 3B-C). Although both patches of membrane shown in Figures 3B and 3E responded similarly to an increase in $[Ca^{2+}]$ from 100 nM (gray curves) to 1 μM (black curves), application of **5r** in the presence of 100 nM Ca^{2+} (blue curve, Figure 3E) shifted the $V_{1/2}$ from 105 mV to -31 mV, an effect that was greater than that caused by a 10-fold increase in $[Ca^{2+}]$. When the $\Delta V_{1/2}$ data from twelve experiments were summarized, **5r** shifted the $V_{1/2}$ (-142 ± 8 mV) significantly more than **5k** (-107 ± 7 mV, $p<0.05$). Compound **5s** did not show any improvement in activity (shifted the $V_{1/2}$ by -137 ± 11 mV) when a methoxy group replaced the methyl group in **5r,** suggesting that the efficacy of these BK channel openers depends more on the hydrophobic nature of the substitution at the *para*-position, rather than its electron donating ability.

Given the difference in efficacy of **5k** and **5r**, we next compared their potencies by constructing concentration effect curves in the continued presence of 100 nM Ca^{2+}. Figure 4A shows a summary concentration effect curve in which the mean $V_{1/2}$ was plotted in the absence and presence of various concentrations of **5k**. The numbers in parentheses refers to

the number of patches exposed to each concentration of **5k**. When these data were fitted with the Hill-Langmuir equation (solid line) a mean EC_{50} of 2.4 μM (95% Confidence Intervals 1.1 μM to 5.3 μM) was obtained. Figure 4B shows a similar experiment in which the effect of increasing concentrations of **5r** were also examined. Similar to the effects of **5k**, **5r** shifted the activation curves in a concentration dependent manner and when these data were fitted with the Hill-Langmuir equation (solid line), it yielded a mean EC_{50} of 2.3 μM (95% Confidence Intervals 1.8 μM to 2.9 μM). This was not significantly different to the results obtained with **5k** and suggests that although **5r** was more efficacious than **5k**, there was little difference in the potency of these two compounds on BK channels. Interestingly, the slope of the concentration effect curve for **5r** (mean Hill slope 1.8; 95% Confidence Intervals 1.2 to 2.5) was steeper than for **5k** (mean Hill slope 0.9; 95% Confidence Intervals 0.4 to 1.3), perhaps suggesting that there was a change in the extent of cooperativity of the binding sites when **5r** was applied.

To illustrate how efficacious the GoSlo-SR family of compounds were, we compared the effects of two well established BK channel openers, NS1619[21] and NS11021[12] on these currents. Figure 5A shows a typical example in which we applied NS1619 (orange line) at a concentration of 10 μM, to a patch containing approximately 23 BK channels. In this example, the activation $V_{1/2}$ was only shifted by ∼−25 mV in the presence of NS1619. In four similar experiments NS1619 shifted the $V_{1/2}$ from 141 ± 6 mV to 116 ± 6 mV as shown in Figure 5B. Application of 10 μM NS1619 shifted the mean $V_{1/2}$ by −23 ± 3 mV (*n*=4), whereas the $\Delta V_{1/2}$ with 10 μM NS11021 in the presence of 100 nM Ca^{2+} was −53 ± 10 mV (*n*=7). In contrast, the five GoSlo-SR compounds shown in the blue bars of Figure 5C shifted the $\Delta V_{1/2}$ in excess of −105 mV (*n*=6-12 patches for each compound). All of these were significantly more effective than either NS compound when compared using ANOVA (p<0.01, Dunnett's post-hoc test).

As mentioned previously, a number of the compounds synthesised here have previously been disclosed as antagonists of purinoceptors (**5a**, **5b**, **5c**, **5j**, **5u**),[16-18] E-NTPDase inhibitors (**5a**, **5b**)[20] or *e*N inhibitors (**5a**, **5i**, **5t**, **5v**).[16-20] However we do not believe that the BK channel agonist activity demonstrated here results from an interaction with purinoceptors or by inhibition of either *e*N or E-NTPDase, for a number of reasons. We have

previously shown that suramin,[11] a non-specific purinoceptor antagonist and *ecto*-ATPase inhibitor has no effect on BK channels when applied (at concentrations up to 1 mM) to the cytosolic surface of BK channels in bladder smooth muscle. Furthermore, **5v**, which has a 2-carboxy-4-fluorophenyl ring as ring D, has previously been shown to potently inhibit *e*N with a K_i of 260 nM,[19] yet failed to significantly alter BK channel activity even at a concentration of 10 μM. Similarly, it appears unlikely that the excitatory effects on BK channels are due to E-NTPDase inhibition since application of an inhibitor of this, ARL67156,[24] even at a concentration of 100 μM (*n*=5), failed to significantly shift the activation $V_{1/2}$ (control 164 ± 8 mV versus 145 ± 6 mV in ARL67156, $\Delta V_{1/2}$=−16 ± 7 mV, p=0.054).

It is equally unlikely that the effects are mediated via an effect on purinoceptors since the SAR of $P2Y_{12}$ antagonists[17] based on AB25, suggest that an acidic group in ring D is essential for this activity. We find that the presence of an acidic group (**5t**) in this ring significantly impaired the ability of the molecules to enhance BK channel opening activity.

Although the binding domain of these compounds on BK channels is not known at present, the above study allows us to hypothesize that some favourable interactions between non-polar groups (isopropyl or benzyl) in *meta*-position of the phenylamino ring and the hydrophobic residues of the receptor could account for the observed activity of **5g** and **5i**. Consistent with this, the lack of efficacy of **5t** and **5u** could be attributed to the reduced lipophilicity in *meta*-position of the D-ring, thus inducing an unfavourable interaction with a specific region of this ion channel. Furthermore, the data from this study also suggest that an acidic group in C-ring is essential for the activity since S175099 failed to significantly alter the activation $V_{1/2}$ of BK channels.

In summary, we have synthesised a series of anthraquinone analogues called the GoSlo-SR family, that act as openers of BK channels and investigated their efficacy in order to obtain initial information about their structure activity relationships. Our data demonstrates that the most efficacious members of the GoSlo-SR family can shift the activation of BK channels in excess of −100 mV, which would activate these channels at physiological potentials, even in the presence of low $[Ca^{2+}]_i$ (100 nM). Further studies to evaluate and develop other lead

structures with the aim of (i) improving the potency in vitro (ii) assessing the efficacy in vivo and (iii) identifying their site of action on BK channels are in progress.

References

[1]   Y. Imaizumi, S. Henmi, Y. Uyama, K. Atsuki, Y. Torii, Y. Ohizumi, M. Watanabe, *Am. J. Physiol*. **1996**, *271*, C772-C782.

[2]   M. A. Hollywood, K. D. McCloskey, N. G. McHale, K. D. Thornbury, *Am. J. Physiol. Cell Physiol*. **2000**, *279*, 420-442.

[3]   B. Kyle, E. Bradley, S. Ohya, G. P. Sergeant, N. G. McHale, K. D. Thornbury, M. A. Hollywood, *Am. J. Physiol. Cell Physiol*. **2011**, *301*, C1186-C2000.

[4]   A. Meredith, K. Thorneloe, M. Werner, M. Nelson, R. Aldrich, *J. Bio. Chem*. **2004**, *279*, 36746-36752.

[5]   I. Milsom, P. Abrams, L. Cardozo, R. G. Roberts, J. Thüroff, A. J. Wein, *BJU Int.* **2001**, *87*, 760-766.

[6]   T. M. Argentieri, J. A. Butera, *Exp. Opin. Ther. Pat.* **2006**, *16*, 573-585.

[7]   M. L. Garcia, D. M. Shen, G. J. Kaczorowski, *Exp. Opin. Ther. Pat.* **2007**, *17*, 831-842.

[8]   A. Nardi, V. Calderone, S. P. Olesen, *Lett. Drug Des. Dis.* **2006**, *3*, 210-218.

[9]   A. Nardi, S. P. Olesen, *Exp. Opin. Ther. Pat.* **2007**, *17*, 1215-1226.

[10]   A. Nardi, S. P. Olesen, *Curr. Med. Chem.* **2008**, *15*, 1126-1146.

[11]   K. Cotton, M. A. Hollywood, K. D. Thornbury, N. G. McHale, *Am. J. Physiol*. **1996**, *270*, C969-C973.

[12]   B. H. Bentzen, A. Nardi, K. Calloe, L. S. Madsen, S. P. Olesen, M. Grunnet, *Mol. Pharmacol*. **2007**, *72*, 1033-1044.

[13]   J. J. Layne, B. Nausch, S. P. Olesen, M. T. Nelson, *Am. J. Physiol. Regul. Integr. Comp. Physiol.* **2010**, *298*, R378-R384.

[14]   H. Knaus, O. McManus, S. Lee, W. Schmalhofer, M. Garcia-Calvo, L. Helms, M. Sanchez, K. Giangiacomo, J. Reuben, A. Smith, G. Kaczorowski, M. Garcia, *Biochemistry* **1994**, *33*, 5819-5828.

[15]   Y. Baqi, C. E. Müller, *Org. Lett.* **2007**, *9*, 1271-1274.

[16]   S. Weyler, Y. Baqi, P. Hillmann, M. Kaulich, A. M. Hunder, I. A. Müller, C. E. Müller, *Bioorg. Med. Chem. Lett.* **2008**, *18*, 223-227.

[17]   Y. Baqi, K. Atzler, M. Köse, M. Glänzel, C. E. Müller, *J. Med. Chem.* **2009**, *52*, 3784-3793.

[18]   Y. Baqi, R. Hausmann, C. Rosefort, J. Rettinger, G. Schmalzing, C. E. Müller, *J. Med. Chem.* **2011**, *54*, 817-830.

[19]   Y. Baqi, S. Y. Lee, J. Iqbal, P. Ripphausen, A. Lehr, A. B. Scheiff, H. Zimmermann, J. Bajorath, C. E. Müller, *J. Med. Chem.* **2010**, *53*, 2076-2086.

[20]   Y. Baqi, S. Weyler, J. Iqbal, H. Zimmermann, C. E. Müller, *Purinergic Signalling* **2009**, *5*, 91-106.

[21]   D. Strøbaek, P. Christophersen, N. R. Holm, P. Moldt, P. K. Ahring, T. E. Johansen, S. P. Olesen, *Neuropharmacology* **1996**, *35*, 903–914.

[22]   C. Kennedy, T. D. Westfall, P. Sneddon, *Semin. Neurosci.* **1996**, *8*, 195–199.

Conflict of Interest Statement

K. D. Thornbury, N. G. McHale, G. P. Sergeant, S. Roy and M. A. Hollywood have submitted a Patent application (IPN WO 2012/035122 A11) on this family of molecules.

Legends

Scheme 1: *Reagents and conditions:* (i) Ar-NH$_2$, Phosphate buffer, Copper powder, microwave, 100-120°C, 5-20 min.

Table 1: *Structure and effect of GoSlo-SR compounds on activation* $\Delta V_{1/2}$. The substituents at each position are given in each column. All compounds were applied at 10 μM to the cytosolic surface of the patch in the presence of 100 nM Ca^{2+}. The change in voltage required for half maximal activation of the channels ($\Delta V_{1/2}$) is shown in the right hand column. Data is quoted as the mean ± standard error of the mean (SEM). Numbers in parentheses represent the number of replicates.

Figure 1. *Structures of Reactive Blue 2 and Acid Blue 25.* Panel A shows the structure of Reactive Blue 2 and Panel B shows the structure of Acid Blue 25.

Figure 2. *Large conductance Ca^{2+}-activated K$^+$ channels in rabbit bladder smooth muscle.*
Upper panels of A-C show voltage ramps from −100 mV to +100 mV were applied in the presence of 100 nM Ca^{2+} (A) and 1 μM Ca^{2+} (B) and from −150 mV to +100 mV in 10 μM Ca^{2+} (C). Increasing Ca^{2+} at the cytosolic surface of the patch increased the number of channel openings and shifted the voltage at which they opened to more negative potentials. This is reflected in Figure 2D which shows the mean activation $V_{1/2}$ in the presence of increasing concentrations of Ca^{2+} at the cytosolic face of the channel. SEM are smaller than the symbol used for means. Figure 2E shows a typical record of the voltage protocol used to evoke BK currents in a patch bathed in 1 μM Ca^{2+} in the absence (Ei) and presence (Eii) of the BK channel blocker penitrem A.

Figure 3. *Comparison of the effects of GoSlo-SR-5-6 and GoSlo-SR-5-44 on the activation of BK channels.* Panels A and D show the structure of GoSlo-SR-5-6 and GoSlo-SR-5-44 respectively. Panels B and E show the effect of 100 nM (grey traces) and 1 μM Ca^{2+} (black traces) on patches before application of 10 μM GoSlo-SR-5-6 and GoSlo-SR-5-44 resepectively in the presence of 100 nM Ca^{2+} (blue traces). Solid lines show Boltzmann fits to the data. Panels C and F show summary bar-charts from 12 separate experiments in which the mean $V_{1/2}$ in the presence of 100 nM Ca^{2+} (grey bars) and 1 μM Ca^{2+} (black bars) on patches before

application of 10μM GoSlo-SR-5-6 (blue bars, Panel C) or 10 μM GoSlo-SR-5-44 (blue bars, Panel F).

Figure 4. *Concentration effect curves for GoSlo-SR-5-6 and GoSlo-SR-5-44.* Panel A shows the mean activation $V_{1/2}$ (±SEM) obtained from patches bathed in 100 nM Ca^{2+} (Control) and in the continued presence of increasing concentrations of GoSlo-SR-5-6. Panel B shows the mean activation $V_{1/2}$ (±SEM) obtained from patches bathed in under control conditions (100 nM Ca^{2+}) and in the continued presence of increasing concentrations of GoSlo-SR-5-44. Numbers in parentheses show the number of experiments at each concentration. The solid lines show the fit to the data obtained with the Hill-Langmuir equation.

Figure 5. *Comparison of Neurosearch compounds with GoSlo-SR compounds.* Panel A shows the effect of 100 nM (grey traces) and 1 μM Ca^{2+} (black traces) on a patch before application of 10 μM NS1619 in the presence of 100 nM Ca^{2+} (orange trace). Solid lines show Boltzmann fits to the data. Panel B shows a summary bar-chart from 4 separate experiments in which the mean $V_{1/2}$ in the presence of 100 nM Ca^{2+} (grey bars) and 1 μM Ca^{2+} (black bars) on patches before application of NS1619 (orange bar). Panel C shows a summary bar-chart in which the mean $\Delta V_{1/2}$ was plotted for two compounds from Neurosearch (NS1619 and NS11021, orange bars) and compared with the effects of five members of the GoSlo-SR family (blue bars) at a concentration of 10 μM.

E = SO$_3$Na (**3**)   E = SO$_3$Na (**5a-v**)
E = CO$_2$H (**4**)   E = CO$_2$H (**6**)
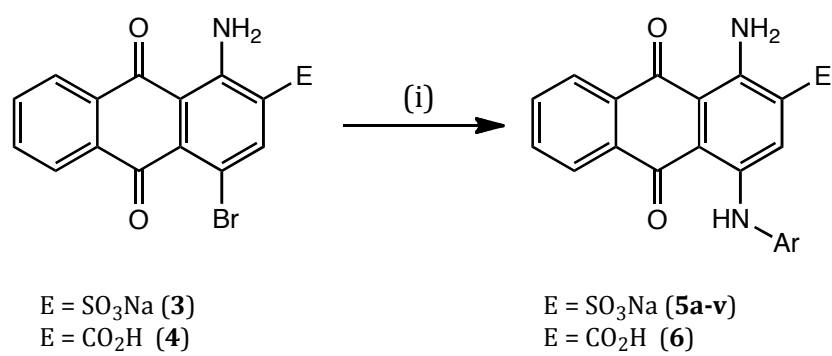
Scheme 1.

Table 1. *Structure and effect of GoSlo-SR compounds on $\Delta V_{1/2}$*
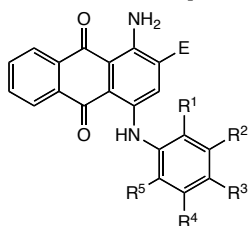
Compound	E	R^1	R^2	R^3	R^4	R^5	$\Delta V_{1/2}$(mV) in 100 nM Ca^{2+}
AB25*	SO_3Na	H	H	H	H	H	−51±10 (*n*=4)
5a*	SO_3Na	H	CH_3	H	H	H	−57±5 (*n*=6)
5b*	SO_3Na	OCH_3	H	H	H	H	−54±15 (*n*=3)
5c*	SO_3Na	C_2H_5	H	H	H	H	−85±9 (*n*=6)
5d	SO_3Na	H	C_2H_5	H	H	H	−92±11 (*n*=9)
5e	SO_3Na	H	H	C_2H_5	H	H	−81±14 (*n*=4)
5f	SO_3Na	$CH(CH_3)_2$	H	H	H	H	−120±8 (*n*=6)
5g	SO_3Na	H	$CH(CH_3)_2$	H	H	H	−113±5 (*n*=7)
5h	SO_3Na	H	H	$CH(CH_3)_2$	H	H	−83±8 (*n*=6)
5i*	SO_3Na	H	CH_2Ph	H	H	H	−120±15 (*n*=6)
5j*	SO_3Na	H	H	CH_2Ph	H	H	−79±5 (*n*=6)
5k	SO_3Na	H	CF_3	H	H	H	−107±7 (*n*=12)
5l	SO_3Na	H	OCF_3	H	H	H	−90±8 (*n*=6)
5m	SO_3Na	H	F	H	H	H	−28±13 (*n*=5)
5n	SO_3Na	H	F	H	F	H	−24±9 (*n*=6)
5o	SO_3Na	F	H	H	H	F	−28±11 (*n*=6)
5p	SO_3Na	H	CF_3	F	H	H	−83±11 (*n*=6)
5q	SO_3Na	H	CF_3	Cl	H	H	−98±12 (*n*=6)
5r	SO_3Na	H	CF_3	CH_3	H	H	−142±8 (*n*=12)
5s	SO_3Na	H	CF_3	OCH_3	H	H	−137±11 (*n*=5)
5t*	SO_3Na	H	CO_2H	H	H	H	−16±9

5u*	SO_3Na	H	NO_2	H	H	H	(n=7) 1±23 (n=3)
5v*	SO_3Na	CO_2H	H	F	H	H	−4±7 (n=5)
6	CO_2H	H	CF_3	H	H	H	−99±11 (n=7)
S175099*	H	H	H	H	H	H	−7±7 (n=7)

Suggested Table of Contents Text:

New BK channel openers: We synthesised a series of anthraquinone analogues, called the GoSlo-SR family. Their effects on bladder smooth muscle BK channels were examined and as shown, shifted voltage dependent activation > -100 mV (at 10 μM). They were more efficacious than NS11021 and may provide a new scaffold for the design of efficacious BK openers.

Suggested Table of Contents Figure:
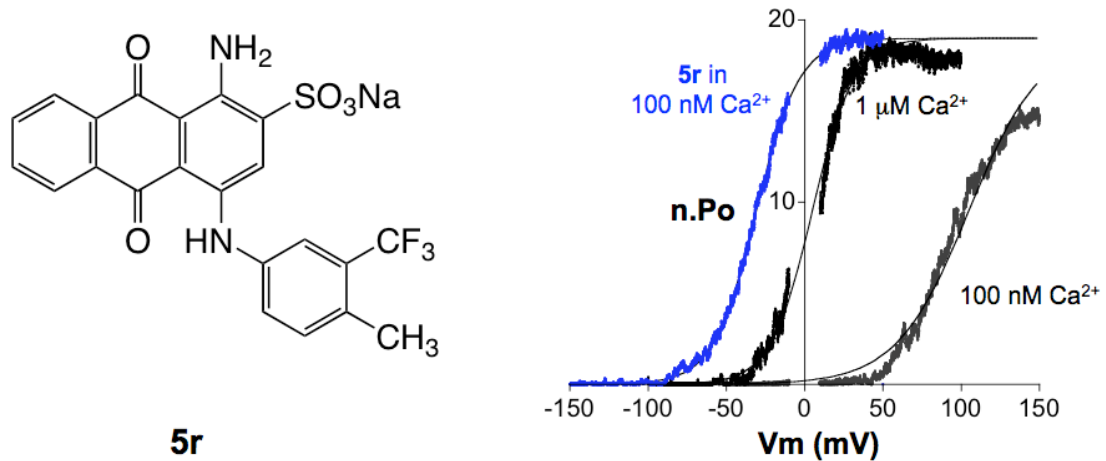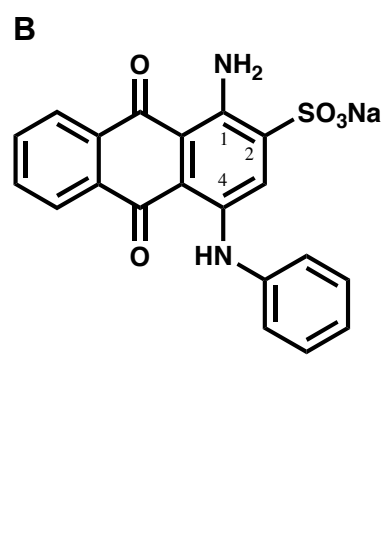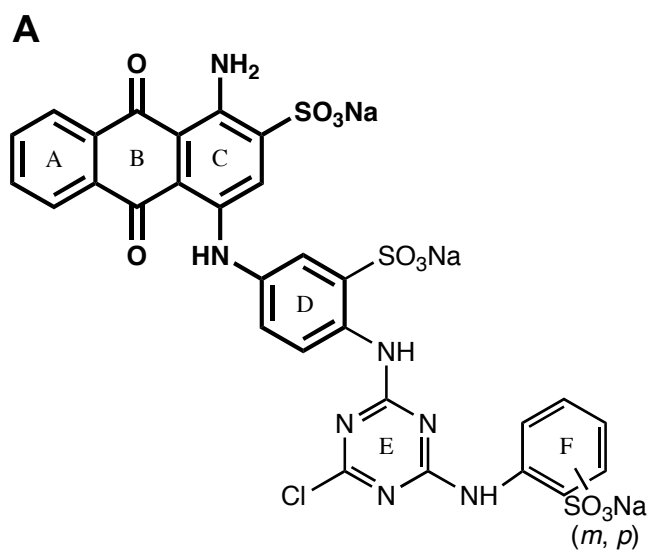
Figure 1. *Structures of Reactive Blue 2 and Acid Blue 25.*

A. 100 nM Ca^{2+}

100 mV

-100 mV

100 pA

500 ms

B. 1 μM Ca^{2+}

100 mV

-100 mV

100 pA

500 ms

C. 10 μM Ca^{2+}

100 mV

-150 mV

100 pA

500 ms

D. Summary data

n=22

$V_{1/2}$ (mV)

150

100

50

0

-50

-100

-150

0.1   1.0   10

[Ca^{2+}] μM

Ei. Control (1 μM Ca^{2+})

100 mV

-100 mV

Eii. Penitrem A (100 nM)

200 pA

200 ms
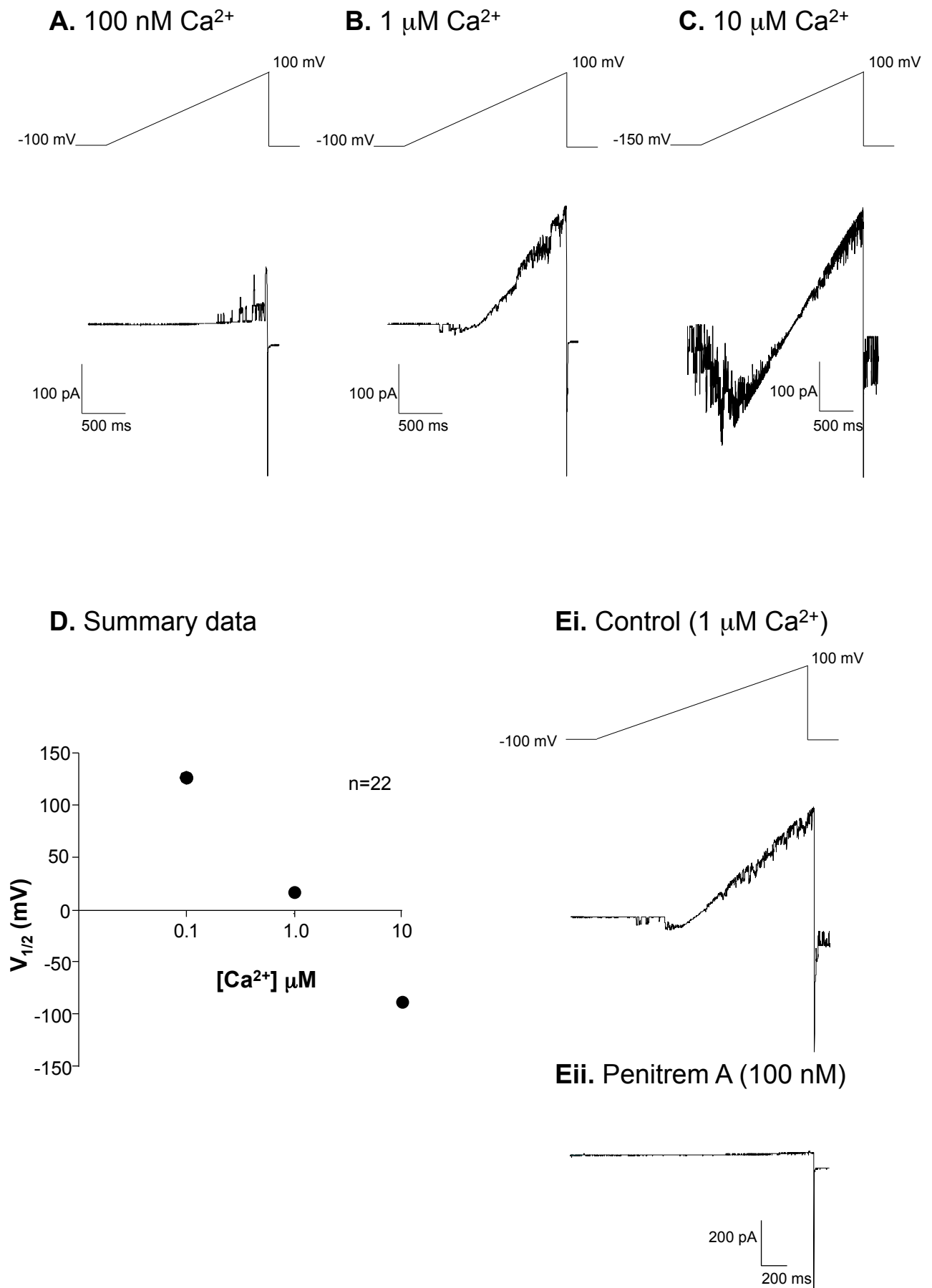
Figure 2. *Large conductance Ca^{2+} activated K$^+$ channels in rabbit bladder smooth muscle.*

A. *GoSlo-SR-5-6 structure (5k)*
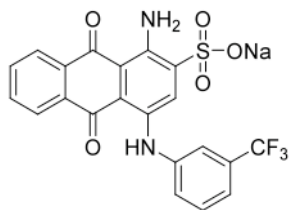
D. *GoSlo-SR-5-44 structure (5q)*
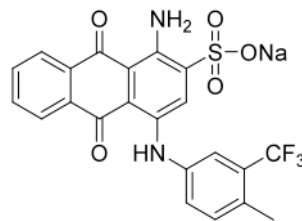
B. *Effect of 10 μM GoSlo-SR-5-6*
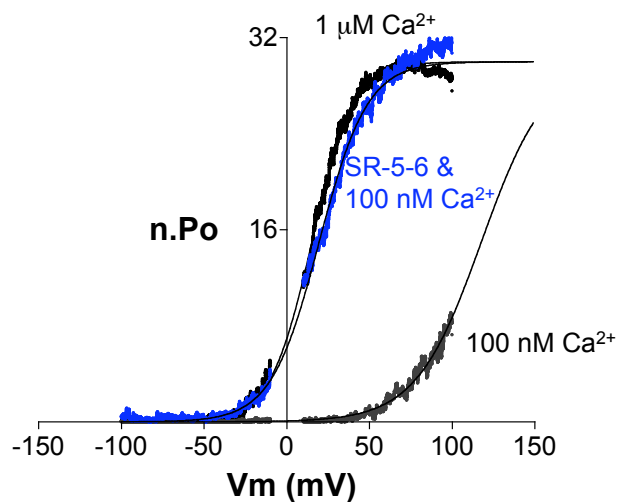
E. *Effect of 10 μM GoSlo-SR-5-44*
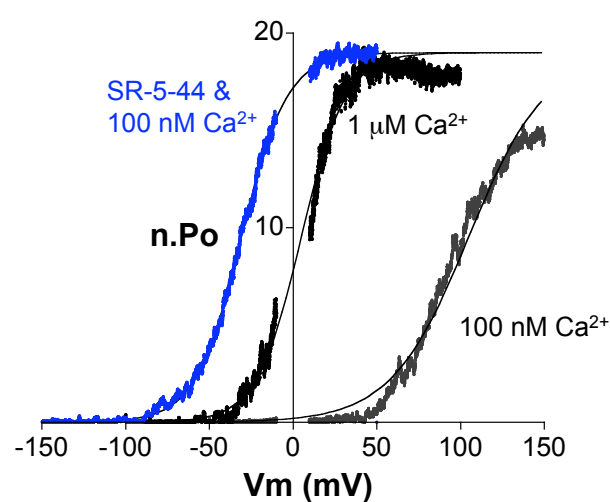
C. *Summary of GoSlo-SR-5-6 on $V_{1/2}$*
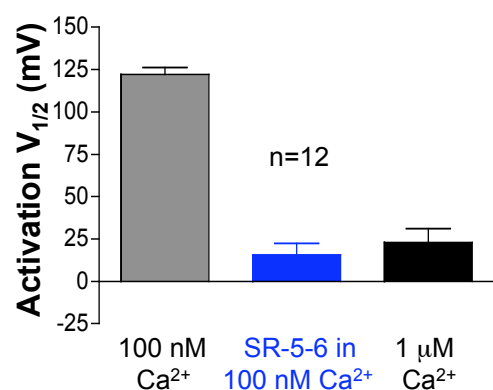
F. *Summary of GoSlo-SR-5-44 on $V_{1/2}$*
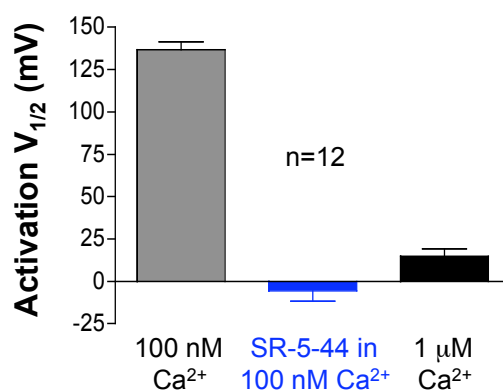
Figure 3. *Comparison of the effects of SR-5-6 and SR-5-44 on BK channels.*

A. GoSlo-SR-5-6
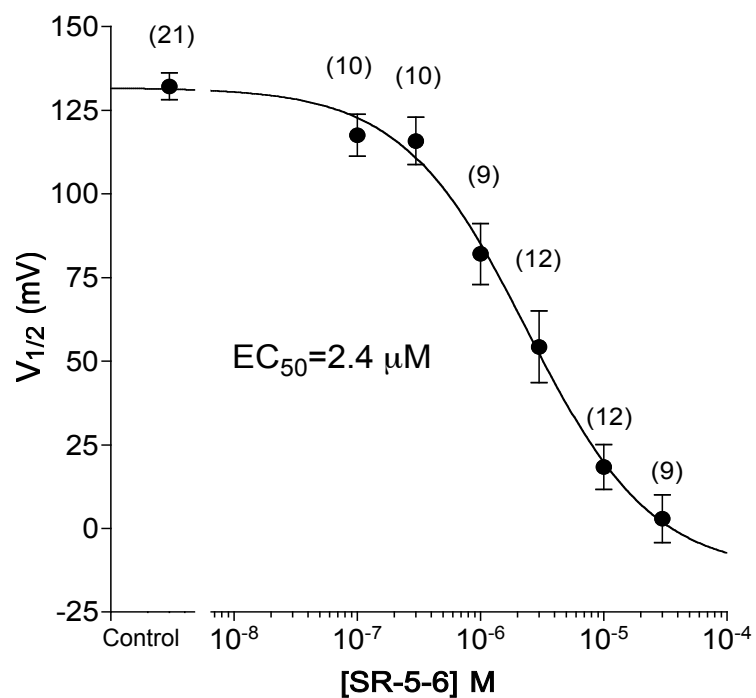
B. GoSlo-SR-5-44
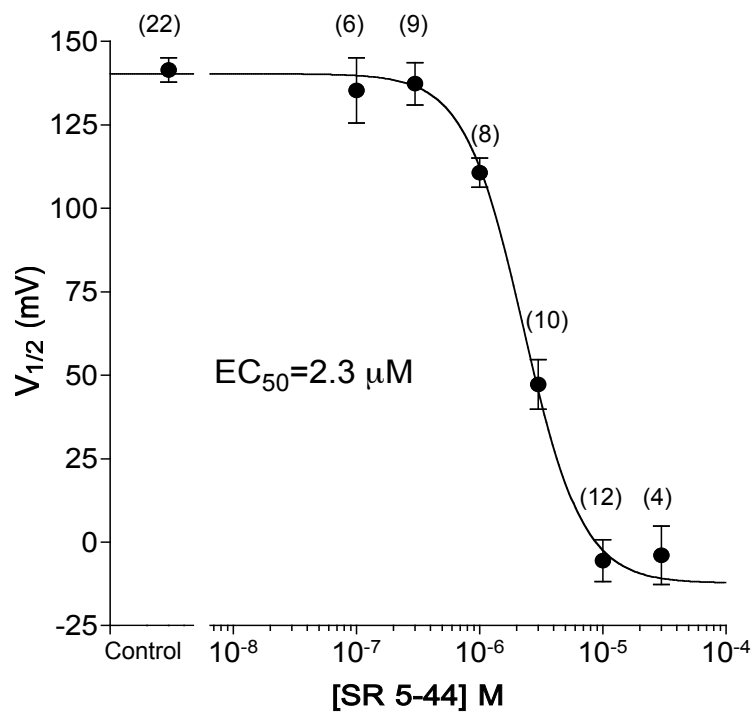
Figure 4. *Concentration effect curves for GoSlo-SR-5-6 and GoSlo-SR-5-44.*

5d   (GoSlo-SR-5-31):   Sodium   1-Amino-4-(3-ethylphenylamino)-9,10-dioxo-9,10-dihydroanthracene-2-sulfonate
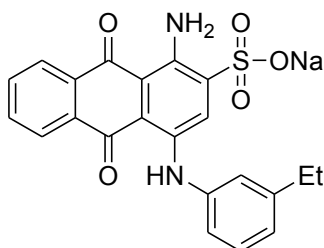
R_f: 0.4 (20% methanol in ethyl acetate).

^{1}H NMR (400 MHz, DMSO-d_6): δ 12.07 (s, 1H), 10.13 (brs, 1H), 8.31-8.23 (m, 2H), 8.08 (s, 1H), 7.87-7.81 (m, 2H), 7.36 (t, *J* = 7.6 Hz, 1H), 7.14 (s, 1H), 7.08 (dd, *J* = 8.0, 20.2 Hz, 2H), 2.64 (ABq, *J* = 7.6 Hz, 2H), 1.22 (t, *J* = 7.6 Hz, 3H).

HRMS (ES): m/z for $C_{22}H_{17}N_2O_5Na_2S$ [M + Na^{+}], calcd. 467.0654, found 467.0666.

5e   (GoSlo-SR-5-97):   Sodium   1-Amino-4-((4-ethylphenyl)amino)-9,10-dioxo-9,10-dihydroanthracene-2-sulfonate
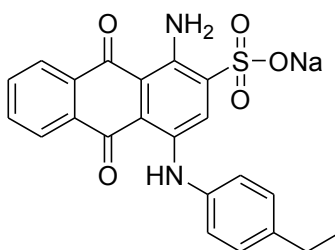
R_f: 0.4 (20% methanol in ethyl acetate).

^{1}H NMR (400 MHz, DMSO-d_6): δ 12.09 (s, 1H), 10.17 (brs, 1H), 8.30-8.26 (m, 2H), 8.00 (s, 1H), 7.88-7.82 (m, 2H), 7.49 (brs, 1H), 7.30 (d, *J* = 8.4 Hz, 2H), 7.21 (d, *J* = 8.8 Hz, 2H), 2.65 (ABq, *J* = 8.0 Hz, 2H), 1.23 (t, *J* = 8.0 Hz, 3H).

HRMS (ES): m/z for $C_{22}H_{17}N_2O_5Na_2S$ [M + Na^{+}], calcd. 467.0654, found 467.0662.

5f   (GoSlo-SR-5-98):   Sodium   1-Amino-4((2-isopropylphenyl)amino)-9,10-dioxo-9,10-dihydroanthracene-2-sulfonate
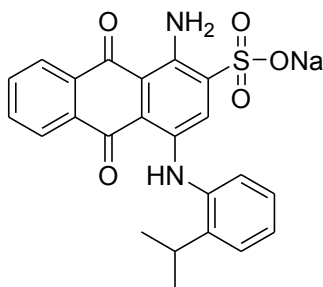
R_f: 0.4 (20% methanol in ethyl acetate).

^{1}H NMR (400 MHz, DMSO-d_6): δ 12.16 (s, 1H), 10.13 (brs, 1H), 8.31-8.29 (m, 2H), 7.89-7.83 (m, 2H), 7.73 (s, 1H), 7.49-7.46 (m, 1H), 7.32-7.24 (m, 3H), 3.23-3.16 (m, 1H), 1.25 (d, J = 7.2 Hz, 6H).

HRMS (ES): m/z for $C_{23}H_{19}N_2O_5Na_2S$ [M + Na$^+$], calcd. 481.0810, found 481.0798.

5g (GoSlo-SR-5-63): Sodium 1-Amino-4-((3-isopropylphenyl)amino)-9,10-dioxo-9,10-dihydroanthracene-2-sulfonate
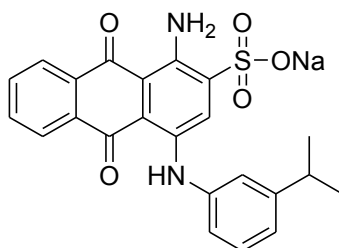
R_f: 0.4 (20% methanol in ethyl acetate).

^{1}H NMR (400 MHz, DMSO-d_6): δ 12.10 (s, 1H), 10.13 (brs, 1H), 8.31-8.25 (m, 2H), 8.10 (s, 1H), 7.88-7.82 (m, 2H), 7.54 (brs, 1H), 7.37 (t, J = 8.0 Hz, 1H), 7.18 (s, 1H), 7.10 (t, J = 7.6 Hz, 2H), 2.96-2.89 (m, 1H), 1.25 (d, J = 6.8 Hz, 6H).

HRMS (ES): m/z for $C_{23}H_{19}N_2O_5Na_2S$ [M + Na$^+$], calcd. 481.0810, found 481.0816.

5h (GoSlo-SR-5-99): Sodium 1-Amino-4-((4-isopropylphenyl)amino)-9,10-dioxo-9,10-dihydroanthracene-2-sulfonate
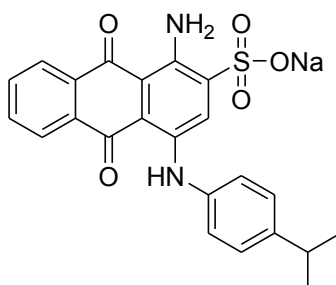
R_f: 0.4 (20% methanol in ethyl acetate).

^{1}H NMR (400 MHz, DMSO-d_6): δ 12.11 (s, 1H), 10.15 (brs, 1H), 8.30-8.27 (m, 2H), 8.02 (s, 1H), 7.88-7.83 (m, 2H), 7.51 (brs, 1H), 7.34 (d, J = 8.4 Hz, 2H), 7.22 (d, J = 8.8 Hz, 2H), 2.97-2.91 (m, 1H), 1.25 (d, J = 6.4 Hz, 6H).

HRMS (ES): m/z for $C_{23}H_{19}N_2O_5Na_2S$ [M + Na$^+$], calcd. 481.0810, found 481.0827.

5i (GoSlo-SR-5-68): Sodium 1-Amino-4-((3-benzylphenyl)amino)-9,10-dioxo-9,10-dihydroanthracene-2-sulfonate
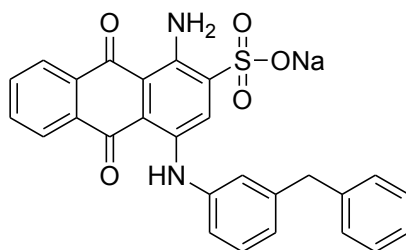
R$_f$: 0.4 (20% methanol in ethyl acetate).

^{1}H NMR (400 MHz, DMSO-d_6): δ 12.05 (s, 1H), 10.12 (brs, 1H), 8.30-8.26 (m, 2H), 8.07 (s, 1H), 7.87-7.84 (m, 2H), 7.51 (brs, 1H), 7.36 (t, J = 7.6 Hz, 1H), 7.32 (s, 2H), 7.31 (s, 2H), 7.21-7.17 (m, 2H), 7.12 (d, J = 8.0 Hz, 1H), 7.05 (d, J = 7.6 Hz, 1H), 3.98 (s, 2H).

HRMS (ES): m/z for $C_{27}H_{19}N_2O_5Na_2S$ [M + Na$^+$], calcd. 529.0810, found 529.0834.

5j (GoSlo-SR-5-37): Sodium 1-Amino-4-(4-benzylphenylamino)-9,10-dioxo-9,10-dihydroanthracene-2-sulfonate
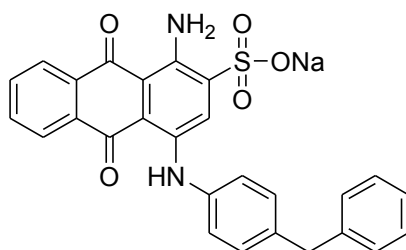
R$_f$: 0.4 (20% methanol in ethyl acetate).

^{1}H NMR (400 MHz, DMSO-d_6): δ 12.07 (s, 1H), 10.11 (brs, 1H), 8.29-8.26 (m, 2H), 8.00 (s, 1H), 7.88-7.81 (m, 2H), 7.34-7.20 (m, 9H), 3.98 (s, 2H).

HRMS (ES): m/z for $C_{27}H_{19}N_2O_5Na_2S$ [M + Na$^+$], calcd. 529.0810, found 529.0812.

5k (GoSlo-SR-5-6): Sodium 1-Amino-9,10-dioxo-4-(3-(trifluoromethyl)phenylamino)-9,10-dihydroanthracene-2-sulfonate
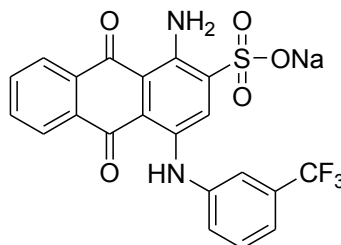
R$_f$: 0.4 (20% methanol in ethyl acetate).

^{1}H NMR (400 MHz, DMSO-d_6): δ 11.80 (s, 1H), 10.02 (brs, 1H), 8.24 (dd, J = 7.2, 13.2 Hz, 2H), 8.04 (s, 1H), 7.85 (m, 2H), 7.65-7.56 (m, 3H), 7.48 (d, J = 7.6 Hz, 1H).

HRMS (ES): m/z for $C_{21}H_{12}N_2O_5F_3S$ [M – Na$^+$], calcd. 461.0419, found 461.0440.

5l (GoSlo-SR-5-34): Sodium 1-Amino-9,10-dioxo-4-(3-(trifluoromethoxy)phenylamino)-9,10-dihydroanthracene-2-sulfonate
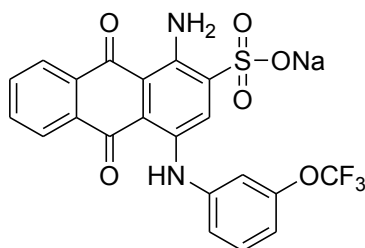
R_f: 0.4 (20% methanol in ethyl acetate).

^{1}H NMR (400 MHz, DMSO-d_6): δ 11.78 (s, 1H), 10.02 (brs, 1H), 8.27-8.22 (m, 2H), 8.07 (s, 1H), 7.89-7.82 (m, 2H), 7.54 (t, J = 8.0 Hz, 1H), 7.31-7.28 (m, 2H), 7.12 (d, J = 8.4 Hz, 1H).

HRMS (ES): m/z for $C_{21}H_{12}N_2O_6F_3Na_2S$ [M + Na$^+$], calcd. 523.0164, found 523.0179.

5m (GoSlo-SR-5-15): Sodium 1-Amino-4-(3-fluorophenylamino)-9,10-dioxo-9,10-dihydroanthracene-2-sulfonate
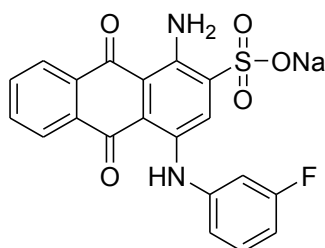
R_f: 0.4 (20% methanol in ethyl acetate).

^{1}H NMR (400 MHz, DMSO-d_6): δ 11.83 (s, 1H), 10.05 (brs, 1H), 8.28-8.23 (m, 2H), 8.06 (s, 1H), 7.89-7.82 (m, 2H), 7.49-7.43 (m, 1H), 7.17-7.11 (m, 2H), 6.99 (dt, J = 2.4, 8.2 Hz, 1H).

HRMS (ES): m/z for $C_{20}H_{12}N_2O_5FS$ [M – Na$^+$], calcd. 411.0451, found 411.0464.

5n (GoSlo-SR-5-11): Sodium 1-Amino-4-(2,6-difluorophenylamino)-9,10-dioxo-9,10-dihydroanthracene-2-sulfonate
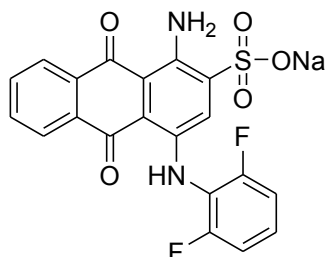
R_f: 0.4 (20% methanol in ethyl acetate).

^{1}H NMR (400 MHz, DMSO-d_6): δ 11.52 (s, 1H), 9.98 (brs, 1H), 8.30-8.27 (m, 2H), 7.89-7.86 (m, 2H), 7.43-7.30 (m, 4H).

HRMS (ES): m/z for $C_{20}H_{11}N_2O_5F_2S$ [M – Na$^+$], calcd. 429.0357, found 429.0348.

5o   (GoSlo-SR-5-28):   Sodium   1-Amino-4-(4-fluoro-3-(trifluoromethyl)phenylamino)-9,10-dioxo-9,10-dihydroanthracene-2-sulfonate
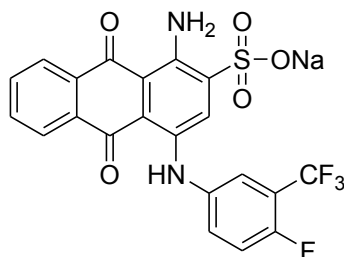
R_f: 0.4 (20% methanol in ethyl acetate).

^{1}H NMR (400 MHz, DMSO-d_6): δ 11.73 (s, 1H), 9.99 (brs, 1H), 8.21 (dd, J = 7.2, 15.2 Hz, 2H), 7.91 (s, 1H), 7.86-7.80 (m, 2H), 7.67-7.63 (m, 2H), 7.57 (t, J = 10.0 Hz, 1H).

HRMS (ES): m/z for $C_{21}H_{11}N_2O_5F_4Na_2S$ [M + Na$^+$], calcd. 525.0120, found 525.0107.

5p   (GoSlo-SR-5-40):   Sodium   1-Amino-4-(4-chloro-3-(trifluoromethyl)phenylamino)-9,10-dioxo-9,10-dihydroanthracene-2-sulfonate
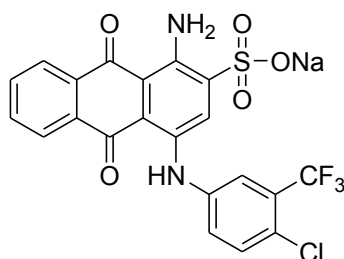
R_f: 0.4 (20% methanol in ethyl acetate).

^{1}H NMR (400 MHz, DMSO-d_6): δ 11.61 (s, 1H), 9.96 (brs, 1H), 8.24-8.17 (m, 2H), 8.00 (s, 1H), 7.87-7.80 (m, 2H), 7.72 (s, 1H), 7.71 (d, J = 12.0 Hz, 1H), 7.54 (dd, J = 2.8, 8.8 Hz, 1H).

HRMS (ES): m/z for $C_{21}H_{11}N_2O_5F_3Na_2SCl$ [M + Na$^+$], calcd. 540.9825, found 540.9824.

5q   (GoSlo-SR-5-44):   Sodium   1-Amino-4-(4-methyl-3-(trifluoromethyl)phenylamino)-9,10-dioxo-9,10-dihydroanthracene-2-sulfonate
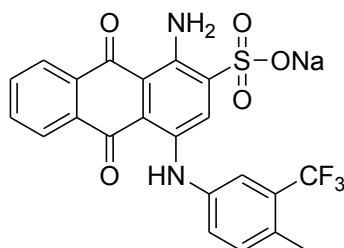
R_f: 0.4 (20% methanol in ethyl acetate).

^{1}H NMR (400 MHz, DMSO-d_6): δ 11.85 (s, 1H), 10.05 (brs, 1H), 8.25-8.20 (m, 2H), 7.97 (s, 1H), 7.86-7.80 (m, 2H), 7.55 (s, 1H), 7.49-7.44 (m, 2H), 2.45 (s, 3H).

HRMS (ES): m/z for $C_{22}H_{14}N_2O_5F_3Na_2S$ [M + Na$^+$], calcd. 521.0371, found 521.0382.

6   **(GoSlo-SR-5-88)**:   1-Amino-9,10-dioxo-4-((3-(trifluoromethyl)phenyl)amino)-9,10-dihydroanthracene-2-carboxylic acid
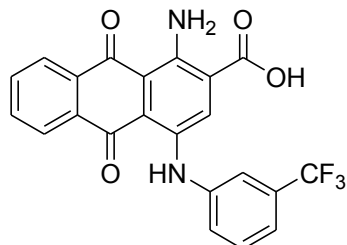
R_f: 0.5 (20% methanol in ethyl acetate).

^{1}H NMR (400 MHz, DMSO-d_6): 11.76 (s, 1H), 10.22 (brs, 2H), 8.33 (s, 1H), 8.28-8.22 (m, 2H), 7.88-7.81 (m, 2H), 7.64-7.59 (m, 3H), 7.44 (d, J = 7.2 Hz, 1H).

HRMS (ES): m/z for $C_{22}H_{14}N_2O_4F_3$ [M + H$^+$], calcd. 427.0906, found 427.0917.

^{1}H NMR spectra of Newly synthesized anthraquinone analogues:
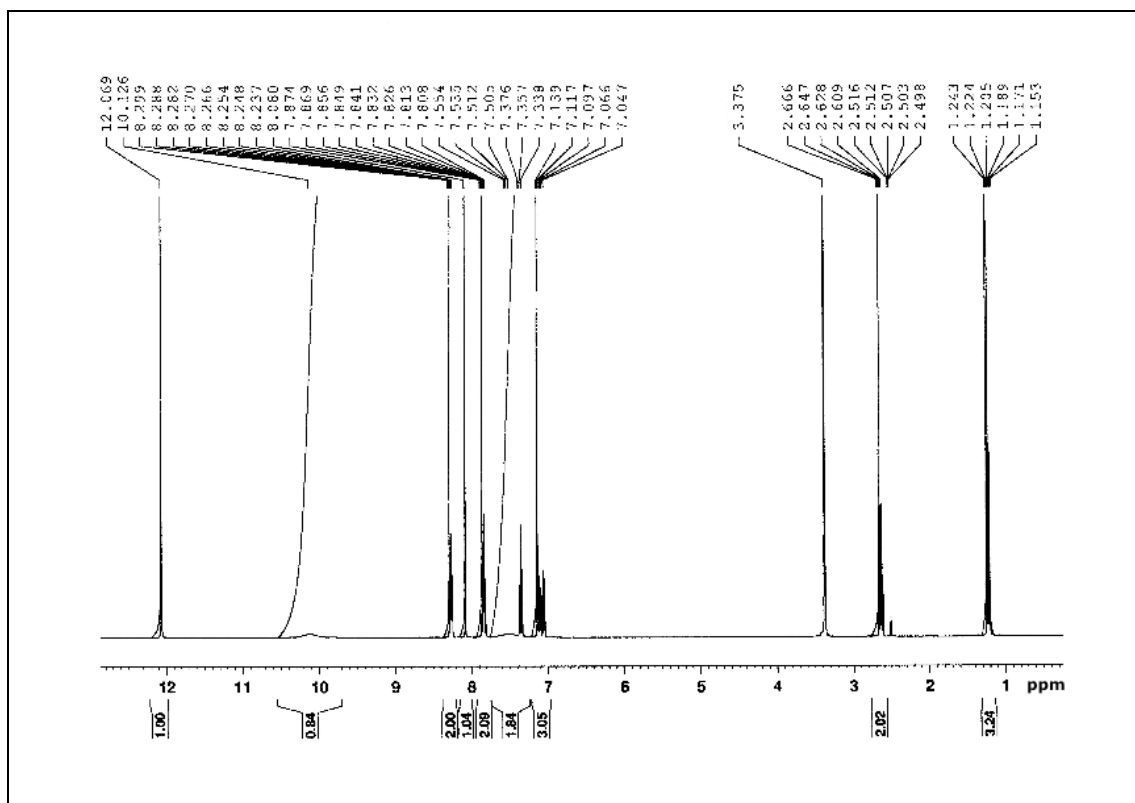
Figure 5: ^{1}H NMR spectrum of **5d** (DMSO-d_6, 400 MHz)
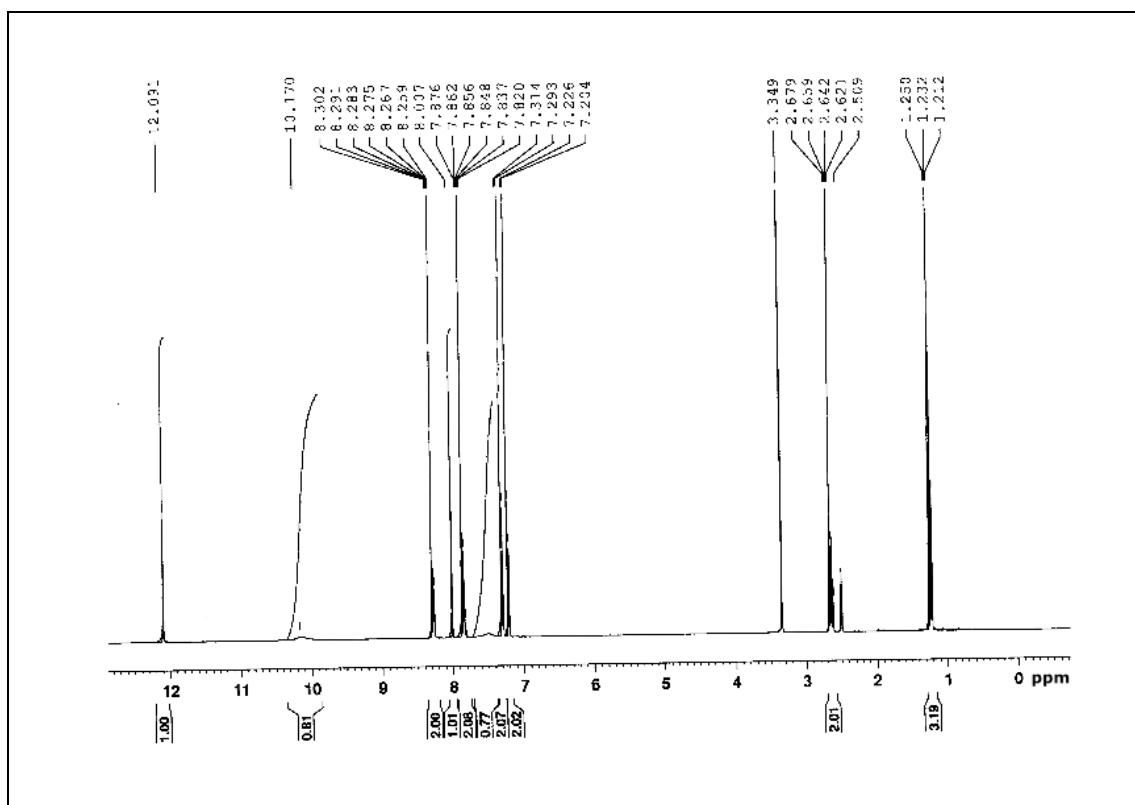
Figure 6: ^{1}H NMR spectrum of **5e** (DMSO-d_6, 400 MHz)
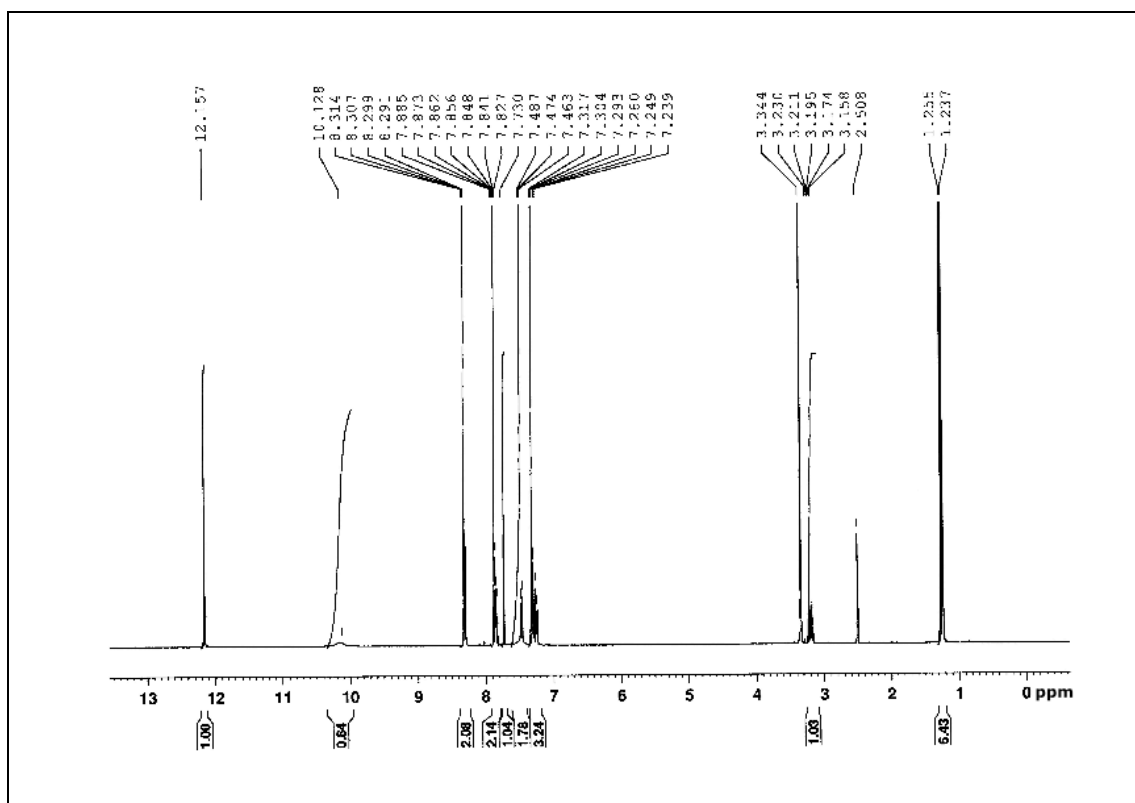
Figure 7: ^{1}H NMR spectrum of **5f** (DMSO-d_6, 400 MHz)
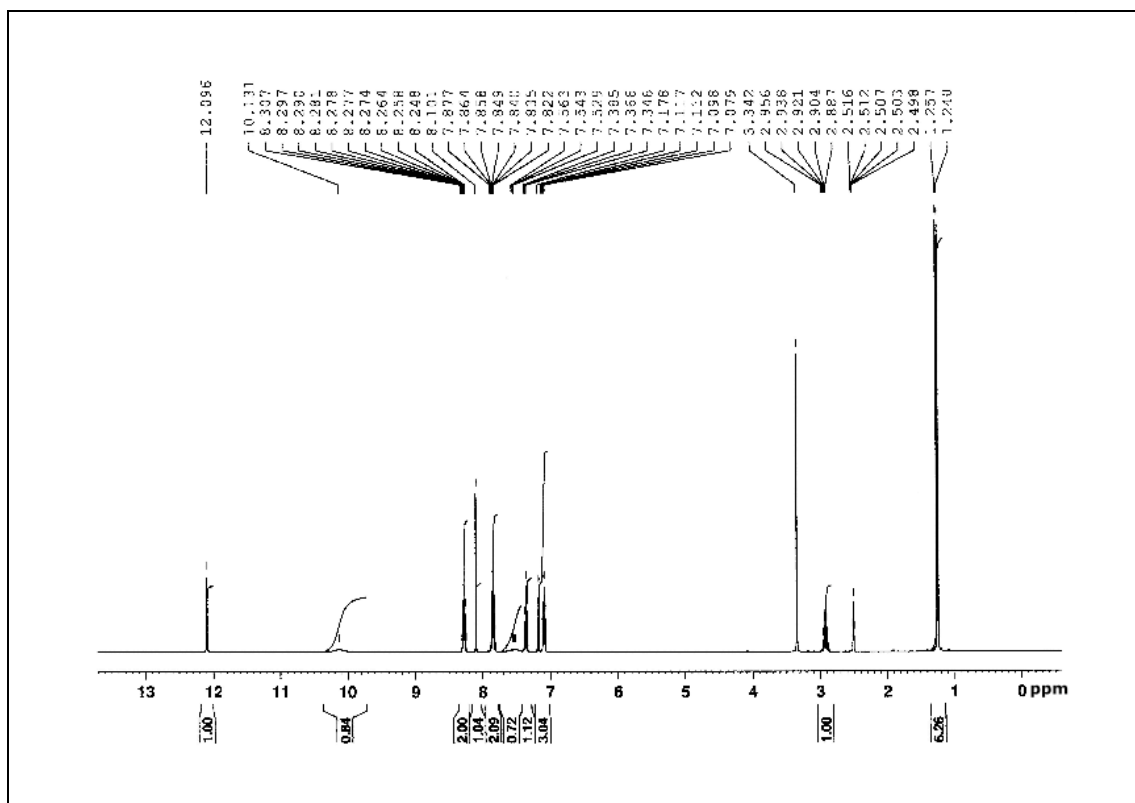
Figure 8: ^{1}H NMR spectrum of **5g** (DMSO-d_6, 400 MHz)
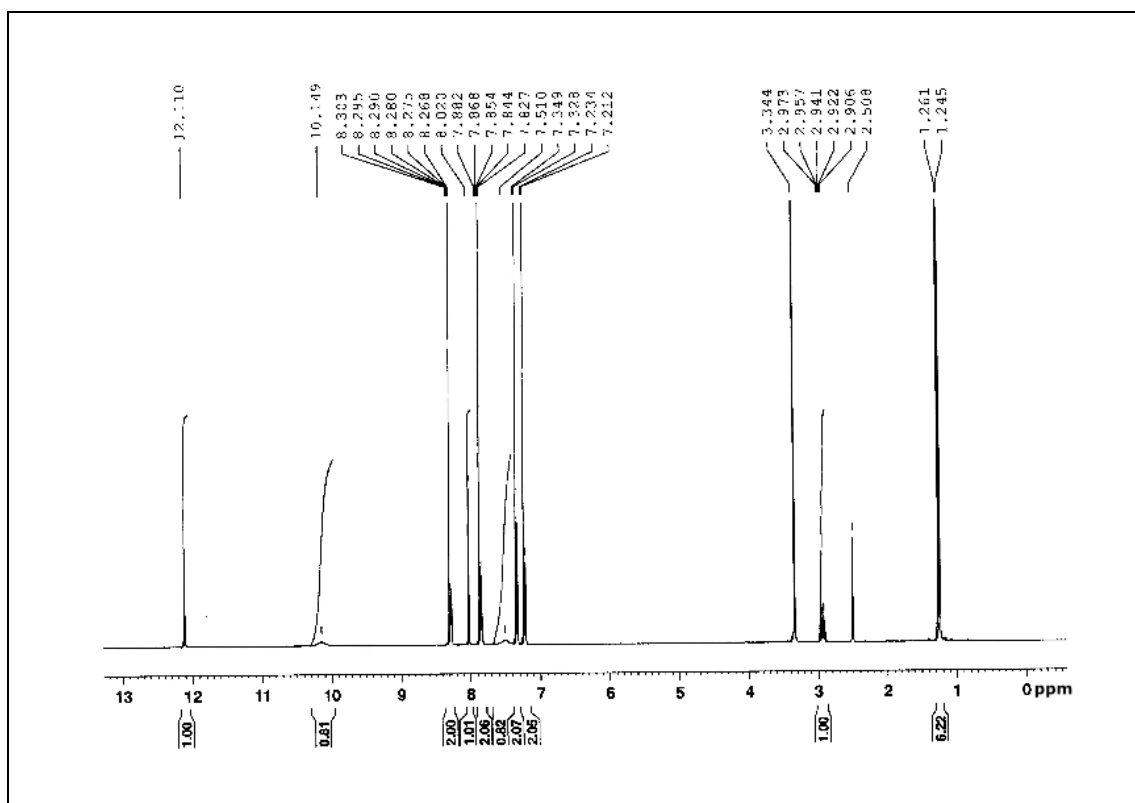
Figure 9: ^{1}H NMR spectrum of **5h** (DMSO-d_6, 400 MHz)
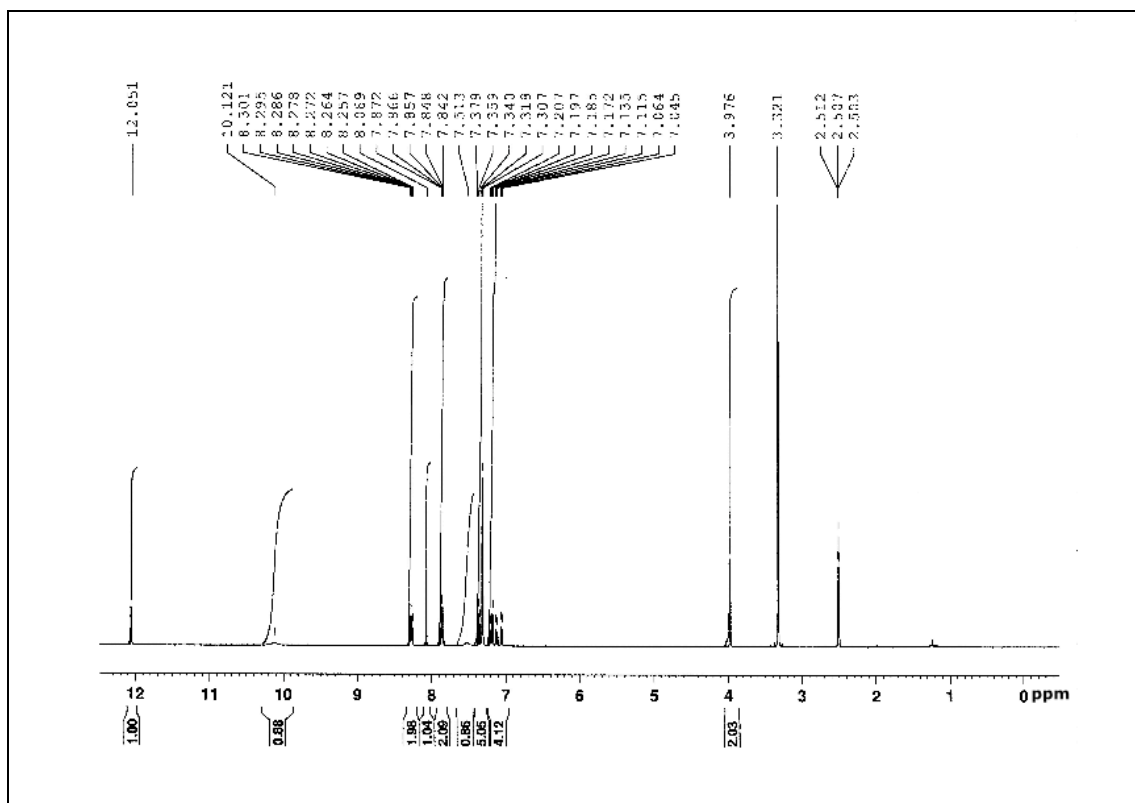
Figure 10: ^{1}H NMR spectrum of **5i** (DMSO-d_6, 400 MHz)
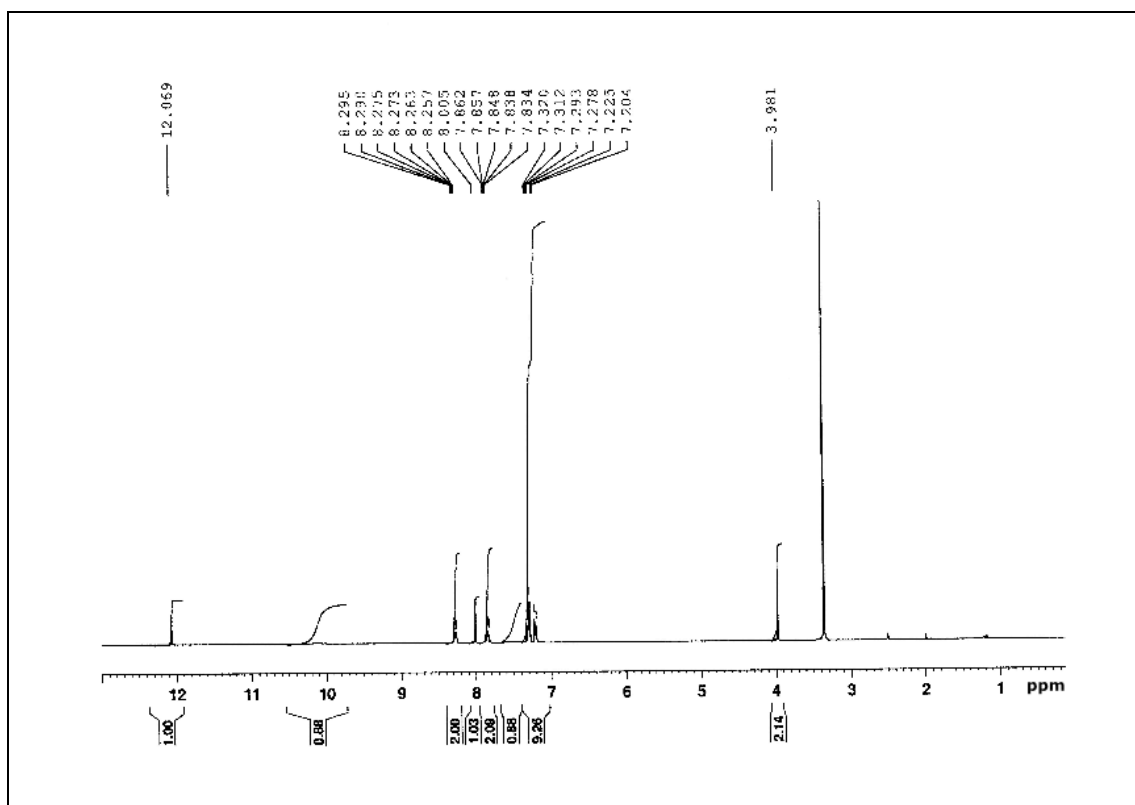
Figure 11: ^{1}H NMR spectrum of **5j** (DMSO-d_6, 400 MHz)
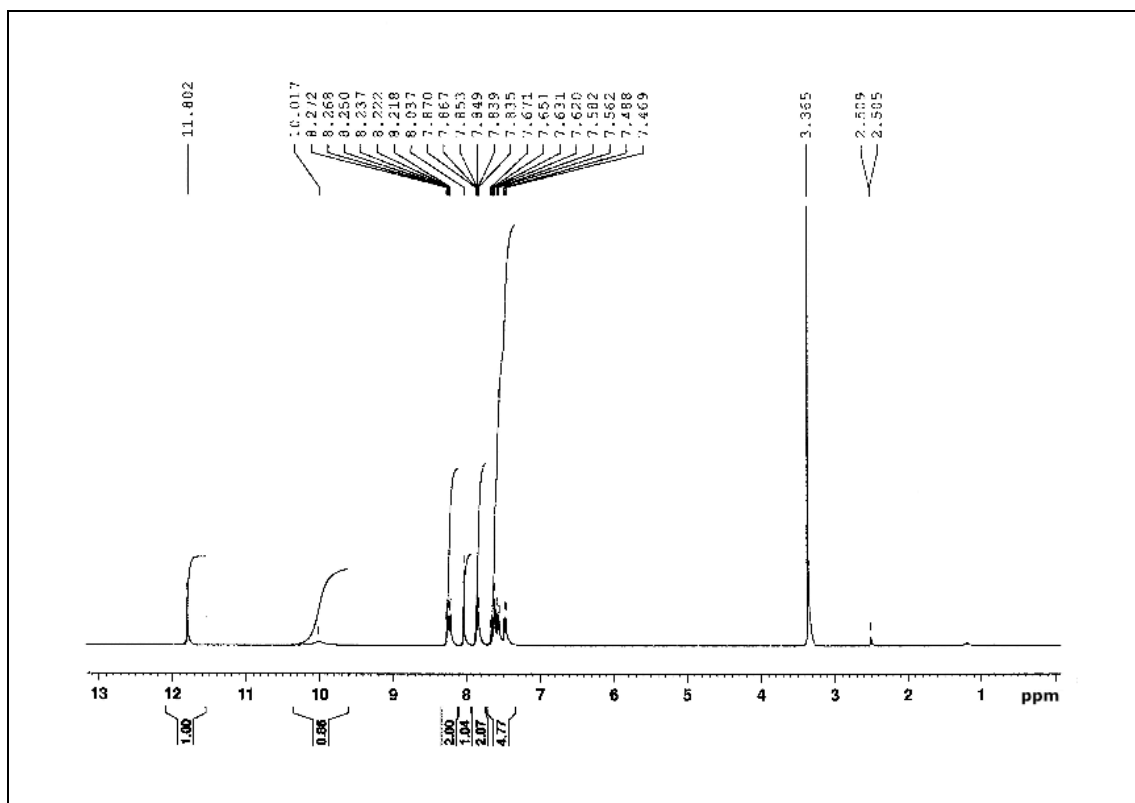
Figure 12: ^{1}H NMR spectrum of **5k** (DMSO-d_6, 400 MHz)
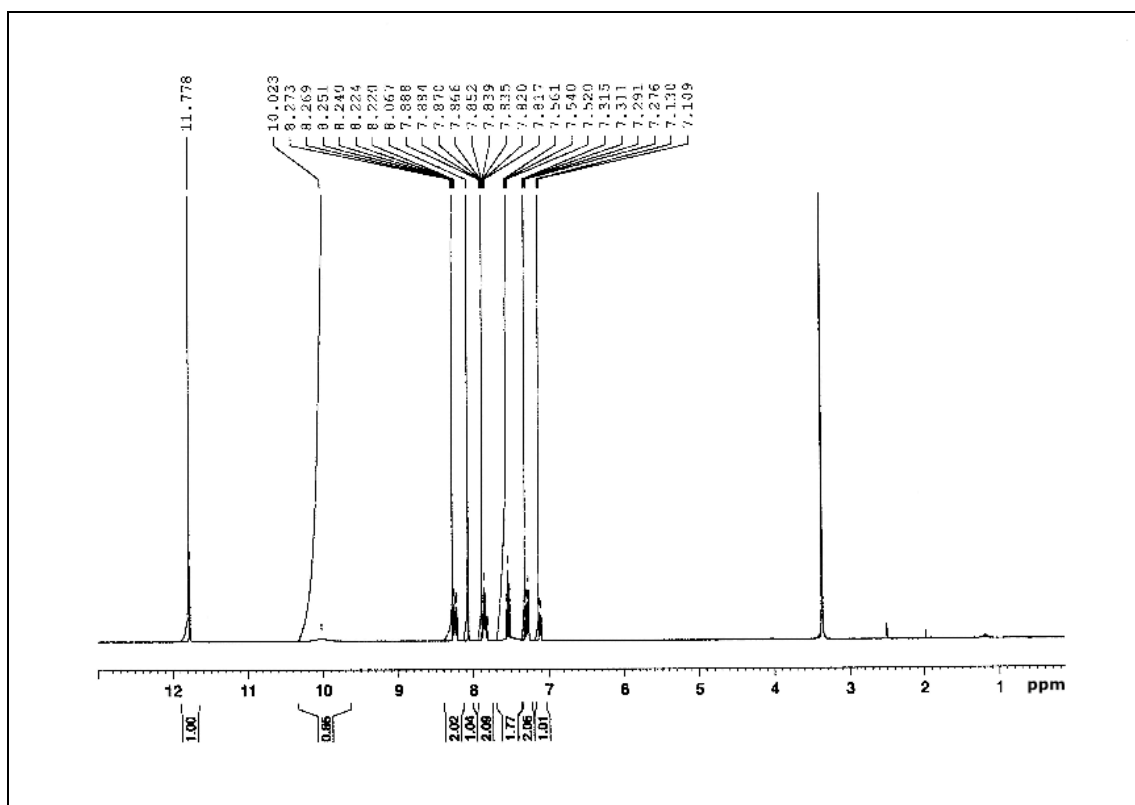
Figure 13: ^{1}H NMR spectrum of **5l** (DMSO-d_6, 400 MHz)
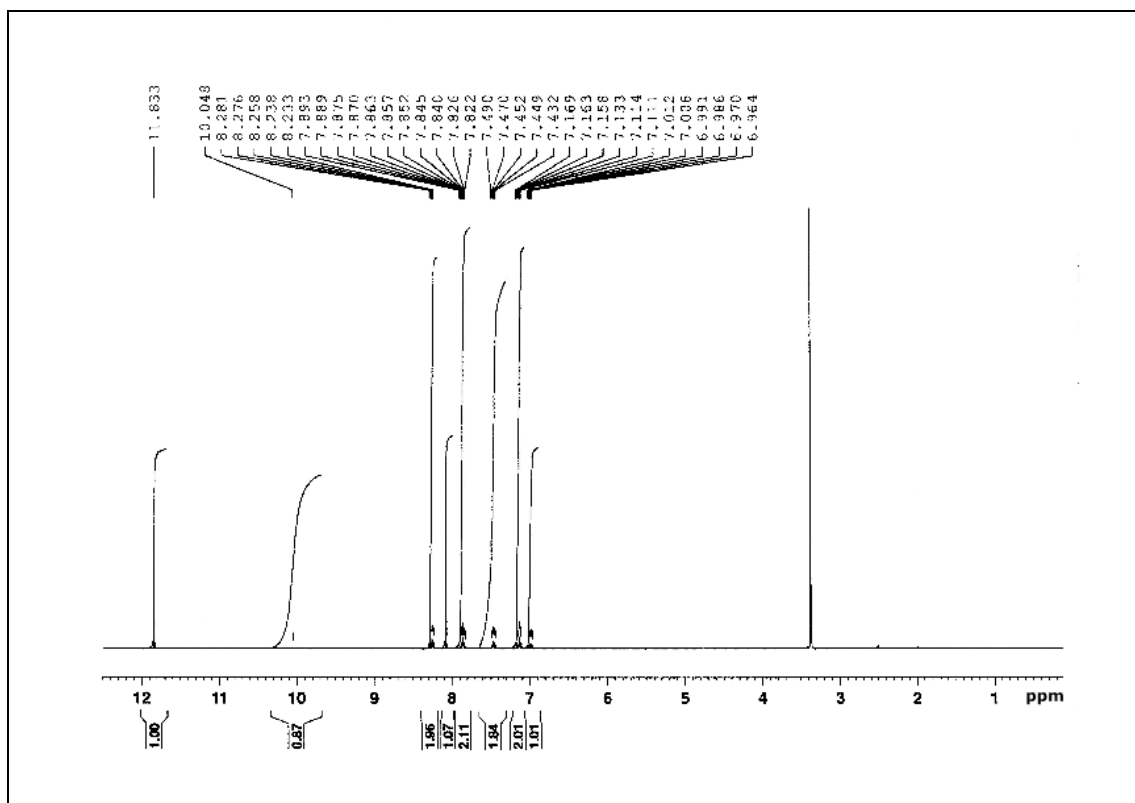
Figure 14: ^{1}H NMR spectrum of **5m** (DMSO-d_6, 400 MHz)
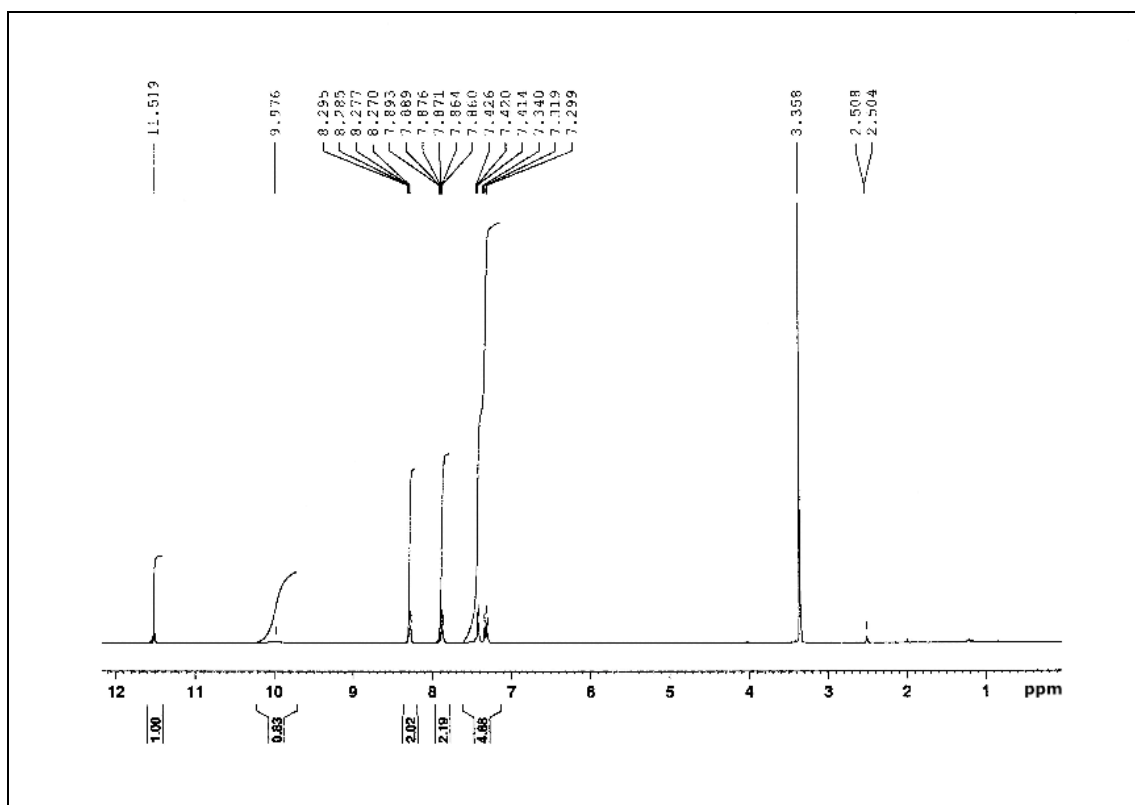
Figure 15: ^{1}H NMR spectrum of **5n** (DMSO-d_6, 400 MHz)
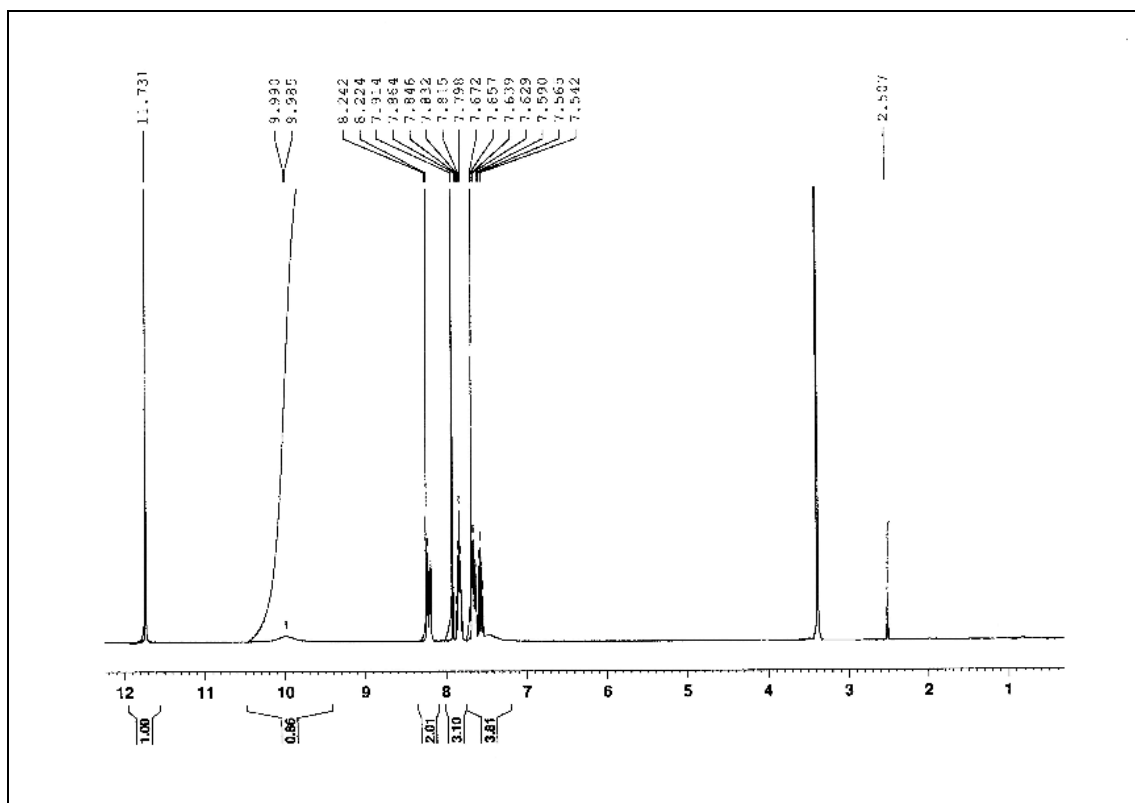
Figure 16: ^{1}H NMR spectrum of **5o** (DMSO-d_6, 400 MHz)
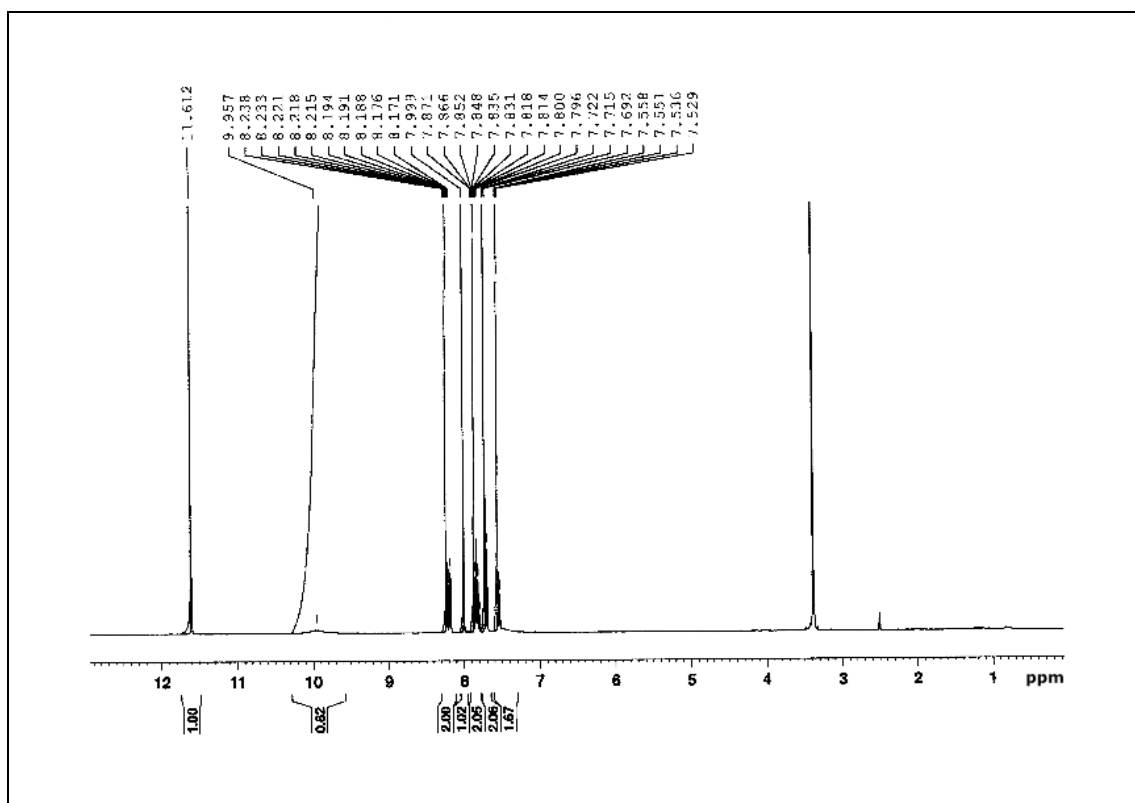
Figure 17: ^{1}H NMR spectrum of **5p** (DMSO-d_6, 400 MHz)
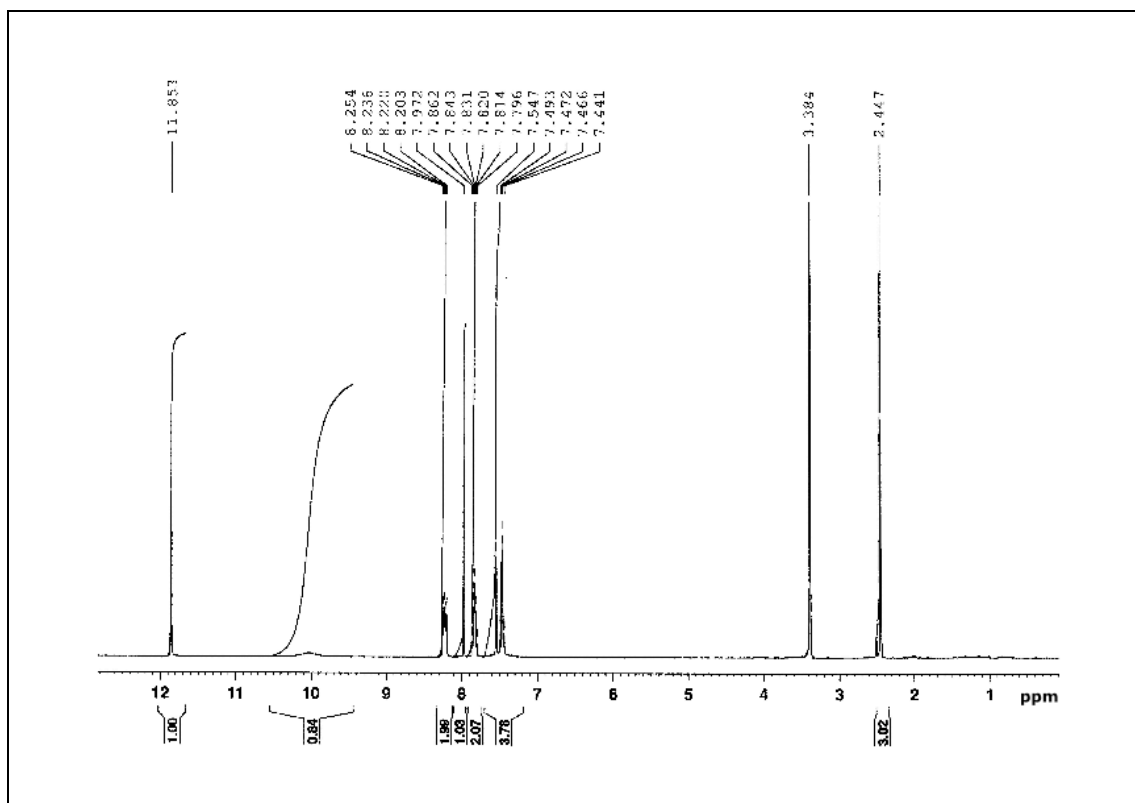
Figure 18: ^{1}H NMR spectrum of **5q** (DMSO-d_6, 400 MHz)
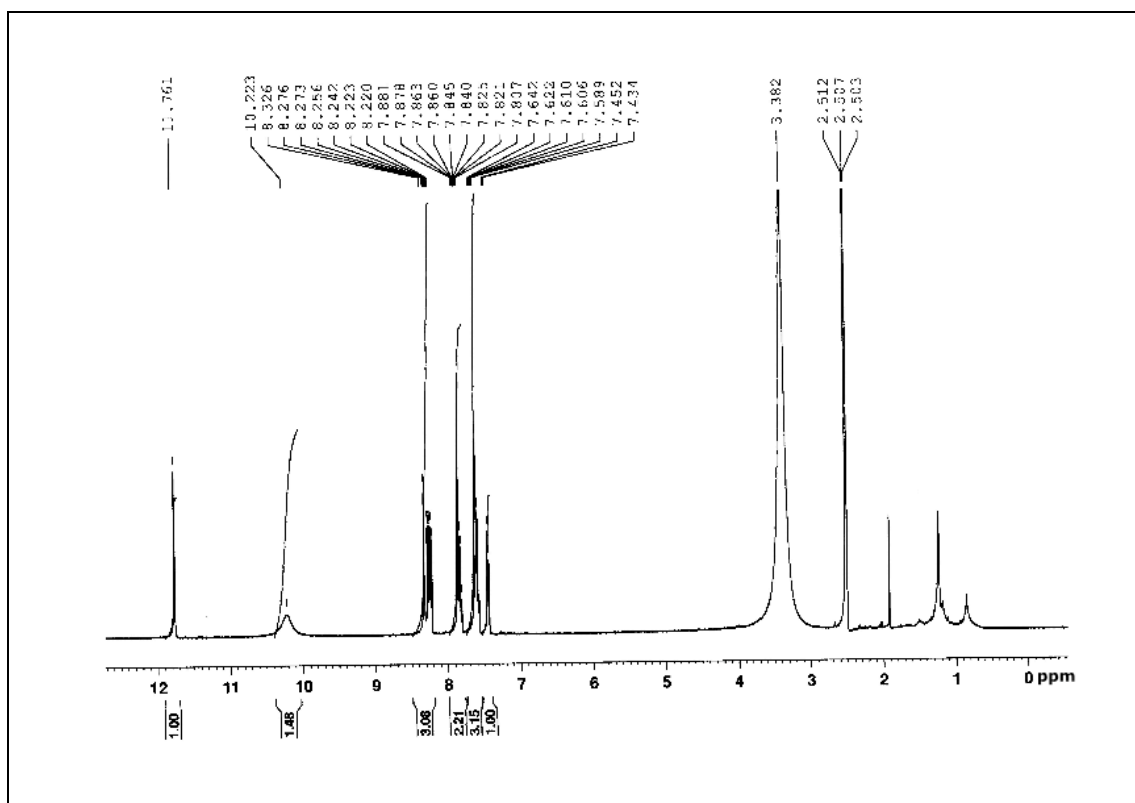
Figure 19: ^{1}H NMR spectrum of **6** (DMSO-d_6, 400 MHz)